

**COMPARATIVE EVALUATION OF SHEAR BOND
STRENGTH OF HEAT POLYMERISED ACRYLIC RESIN
TO SURFACE TREATED COBALT-CHROMIUM AND
TITANIUM ALLOYS - AN IN VITRO STUDY**

Dissertation Submitted to
THE TAMILNADU DR. M.G.R. MEDICAL UNIVERSITY

In partial fulfillment for the Degree of
MASTER OF DENTAL SURGERY



BRANCH I
PROSTHODONTICS AND CROWN & BRIDGE
APRIL 2012

CERTIFICATE

This is to certify that the dissertation titled “COMPARATIVE EVALUATION OF SHEAR BOND STRENGTH OF HEAT POLYMERISED ACRYLIC RESIN TO SURFACE TREATED COBALT-CHROMIUM AND TITANIUM ALLOYS - AN IN VITRO STUDY” is a bonafide record work done by **Dr.B.SIVA SARANYA** under our guidance and to our satisfaction during her post graduate study period between 2009 – 2012.

This Dissertation is submitted to **THE TAMILNADU DR. M.G.R. MEDICAL UNIVERSITY**, in partial fulfillment for the Degree of **MASTER OF DENTAL SURGERY – PROSTHODONTICS AND CROWN & BRIDGE, BRANCH I**. It has not been submitted (partial or full) for the award of any other degree or diploma.

Guided by


Dr. N.S. Azhagarasan, M.D.S.,

Professor and Head of the Department,
Department of Prosthodontics
and Crown & Bridge,
Ragas Dental College & Hospital
Chennai.

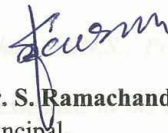
PROFESSOR & HEAD
DEPT OF PROSTHODONTICS
Ragas Dental College & Hospital
Chennai - 600 113.





Dr. K. Chitra Shankar, M.D.S.,

Professor,
Department of Prosthodontics
and Crown & Bridge,
Ragas Dental College & Hospital
Chennai.



Dr. S. Ramachandran, M.D.S.,
Principal,
Ragas Dental College & Hospital,
Chennai.



PRINCIPAL
RAGAS DENTAL COLLEGE & HOSPITAL
CHENNAI

ACKNOWLEDGEMENT

*First of all, I would like to thank **Almighty God** for giving me the strength, courage and confidence to overcome all hurdles and finish this arduous job.*

This dissertation is the result of work with immense support from many people and it is my pleasure to take this opportunity to express my gratitude to all of them.

*I would be failing in my duty if I do not adequately express my deep sense of gratitude and my sincere thanks to **Dr. N. S. Azhagarasan, M.D.S., Professor and Head of the Department, Department of Prosthodontics and Crown & Bridge, Ragas Dental College and Hospital, Chennai**, for his exceptional guidance, tremendous encouragement and well timed suggestions throughout my postgraduate programme. I would like to profoundly thank him for giving an ultimate sculpt to this study.*

*I wish to express my gratitude to **Dr. S Ramachandran, M.D.S., Principal, Ragas Dental College, Chennai** for his encouragement and support throughout my post graduate course. I also thank him for permitting me to make use of the amenities in the institution.*

*I would like to express my real sense of respect, gratitude and thanks to my **Guide, Dr. K. Chitra Shankar, M.D.S., Professor** for her guidance, constant support and encouragement extended to me during this study. Her patience and perseverance benefited me in every facet of my study and I thoroughly enjoyed every discussion with her. Her valuable guidance and positive criticisms enabled*

me to develop an understanding of the subject from the concept to the conclusion. Her guidance and supervision helped me to bring the best out of me in this study. The timely help and encouragement rendered by her had been enormously helpful throughout my study.

*I would also like to thank **Dr. K. Madhusudan, M.D.S., Dr.S. Jayakrishnakumar, M.D.S., Dr. Manoj Rajan, M.D.S. and Dr. Saket Miglani, M.D.S.,** for their valuable suggestions and support given throughout my study.*

*My sincere thanks to **Dr. Manikandan, M.D.S., Dr.R. Hariharan, M.D.S., Dr.M.Saravana Kumar, M.D.S., Dr.Vallabh Mahadevan, M.D.S., Dr.Sabarinathan, M.D.S., Dr.Divya Krishnan, M.D.S.,** for their support during this study.*

*I would like to thank **Professor Dr.N. Kalyana Krishnan,** Sree Chitra Tirunal Institute for Medical Sciences And Technology, Thiruvananthapuram, for helping me in thermocycling procedure.*

*I would like to convey my sincere thanks to **Professor Mr.N.Karthikeyan,** and **Mr.D.Balamurugan,** Department of Mechanical Engineering, Central Institute of Plastic Engineering and Technology, Chennai, for their help and support throughout the study.*

*I would like to convey my gratitude to **Professor Mr.Srinivasan and Mr.Babu,** Department of Mechanical Engineering, Anna University, Guindy, Chennai for helping me in Scanning Electron Microscopic analysis.*

*I would like to thank **Mr.Sakthinathan**, Assistant Professor and **Mr.Vetrivel**, Technical Assistant, Department of Manufacturing Engineering for helping me in the Surface Profilometric analysis.*

*My thanks to **Ms.S.Deepa**, Statistician, Department of Oral Pathology, Ragas Dental College and Hospital, Chennai, for her valuable help with the statistical work for this study.*

It would not be justifiable on my part if I do not acknowledge the help of my fellow colleagues, my seniors, juniors and friends for their constant encouragement and continued support throughout my post graduate course.

*Last but not the least, even though words would not do much justice, I would like to specially thank my husband, parents, my brother and my daughter **Harsika sree** for their love and support.*

CONTENTS

Title	Page No
1. INTRODUCTION	1
2. REVIEW OF LITERATURE	9
3. MATERIALS AND METHODS	21
4. RESULTS	43
5. DISCUSSION	49
6. CONCLUSION	64
7. SUMMARY	70
8. BIBLIOGRAPHY	73

LIST OF TABLES

Table No.	Title	Page No.
1	Basic values and Mean value of shear bond strength in Mpa for acrylised samples of Group Ia.	45
2	Basic values and Mean value of shear bond strength in Mpa for acrylised samples of Group Ib.	45
3	Basic values and Mean value of shear bond strength in Mpa for acrylised samples of Group IIa.	46
4	Basic values and Mean value of shear bond strength in Mpa for acrylised samples of Group IIb.	46
5	Comparison of Mean shear bond strengths of Group Ia with Group Ib	47
6	Comparison of Mean shear bond strengths of Group IIa with Group IIb	47
7	Comparison of Mean shear bond strengths of Group Ia with Group IIa	48
8	Comparison of Mean shear bond strengths of Group Ib with Group IIb	48

ANNEXURE
LIST OF FIGURES

Fig.No.	Title
Fig 1a:	Line diagram showing assembled custom made mold
Fig 1b-f:	Line diagram of individual custom made mold parts
Fig 2:	Custom-made mold
Fig 3:	Petroleum jelly
Fig 4:	Pattern resin
Fig 5a:	Inlay wax
Fig 5b:	Preformed mesh pattern
Fig 6:	Sprue wax
Fig 7:	Surfactant spray
Fig 8:	Silicon casting ring
Fig 9:	Phosphate bonded investment
Fig 10:	Alumina and Magnesia based investment
Fig 11:	Investment liquid
Fig 12:	Co-Cr alloy
Fig 13:	Ti-6Al-4V alloy
Fig 14a:	Aluminium oxide powder 250 μ m
Fig 14b:	Aluminium oxide powder 50 μ m
Fig 15:	Modelling wax
Fig 16:	Model plaster

Fig 17a:	Separating medium
Fig 17b:	Heat cure acrylic resin
Fig 18:	Alloy Primer
Fig 19a:	Separating discs
Fig 19b:	Rubber polishing wheel
Fig 20:	Wax solvent
Fig 21a:	Sandpaper of different grit sizes
Fig 21b:	Pumice
Fig 22:	Distilled water
Fig 23:	PKT instrument
Fig 24a:	Stainless steel metal scale
Fig 24b:	Wax caliper
Fig 24c:	Metal caliper
Fig 25a:	Porcelain cup
Fig 25b:	Measuring jar
Fig 26a:	Wax knife
Fig 26b:	Wax carver
Fig 26c:	Stainless steel spatula
Fig 27:	Rubber bowl
Fig 28a:	Metal trimmers and disc mandrel
Fig 28b:	Acrylic trimmers
Fig 28c:	Sandpaper mandrel
Fig 29:	Denture flask and dental clamp
Fig 30:	Vacuum power mixer

Fig 31:	Burnout furnace
Fig 32:	Crucible
Fig 33:	Induction casting machine
Fig 34:	Casting machine for titanium
Fig 35:	Sandblaster
Fig 36:	Alloy grinder
Fig 37:	Dental lathe
Fig 38:	Acryliser
Fig 39:	Steam cleanser
Fig 40:	Plastic containers
Fig 41:	Incubator
Fig 42:	Thermocycler
Fig 43:	Universal testing machine
Fig 44:	Surface Profilometer
Fig 45:	Scanning Electron Microscope
Fig 46a,b:	Schematic diagram showing sample pattern dimensions
Fig 46c:	Patterns with a space in the centre
Fig 46d:	Preformed mesh patterns
Fig 46e:	Finished sample patterns
Fig 47:	Sprue attached patterns
Fig 48:	Investment mold
Fig 49:	Retrieved casting
Fig 50:	Finished Co-Cr alloy samples
Fig 51:	Sprue attached wax pattern for titanium casting

- Fig 52: Finished Ti-6Al-4V alloy samples
- Fig 53a: Line diagram showing cylindrical acrylic extension dimensions
- Fig 53b: Line diagram showing waxed-up alloy sample
- Fig 53c: Waxed up alloy samples
- Fig 54: Invested waxed up samples
- Fig 55: Denture flask carrying the cylindrical mold spaces for acrylic and alloy samples in the flask base
- Fig 56a: Air abraded alloy samples
- Fig 56b: Alloy primer application
- Fig 57: Deflasked samples
- Fig 58: Finished samples
- Fig 59a: Samples in the separate, labeled containers
- Fig 59b: Samples in the incubator
- Fig 60: Samples in the thermocycler
- Fig 61: Sample fixed in the sample fixture of universal testing machine
- Fig 62: Tested samples
- Fig 63: Samples in gold sputtering machine prior to SEM

LIST OF GRAPHS

Graph No:	Title
Graph 1	Basic values of shear bond strength (in Mpa) for Group Ia
Graph 2	Basic values of shear bond strength (in Mpa) for Group Ib
Graph 3	Basic values of shear bond strength (in Mpa) for Group IIa
Graph 4	Basic values of shear bond strength (in Mpa) for Group IIb
Graph 5	Comparison of mean shear bond strength values of Group Ia, Ib, IIa and IIb
Graph 6	Comparison of shear bond strength values of Group Ia with Group Ib
Graph 7	Comparison of mean shear bond strength values of Group Ia with Group Ib
Graph 8	Comparison of shear bond strength values of Group IIa with Group IIb
Graph 9	Comparison of mean shear bond strength values of Group IIa with Group IIb
Graph 10	Comparison of shear bond strength values of Group Ia with Group IIa
Graph 11	Comparison of mean shear bond strength values of Group Ia with Group IIa
Graph 12	Comparison of shear bond strength values of Group Ib with Group IIb
Graph 13	Comparison of mean shear bond strength values of Group Ib with Group IIb

LIST OF SURFACE PROFILOMETRY PHOTOMICROGRAPHS

Fig.No.	Title
Fig 64:	3-D image of Group Ia
Fig 65:	Advanced 3-D image of Group Ia
Fig 66:	3-D image of Group Ib
Fig 67:	Advanced 3-D image of Group Ib
Fig 68:	3-D image of Group IIa
Fig 69:	Advanced 3-D image of Group IIa
Fig 70:	3-D image of Group IIb
Fig 71:	Advanced 3-D image of Group IIb

LIST OF SEM PHOTOMICROGRAPHS

Fig No.	Title
Fig 72:	SEM photomicrograph of Group Ia pretest SEM under 10x
Fig 73:	SEM photomicrograph of Group Ib pretest SEM under 10x
Fig 74:	SEM photomicrograph of Group Ia pretest SEM under 500x
Fig 75:	SEM photomicrograph of Group Ib pretest SEM under 500x
Fig 76:	SEM photomicrograph of Group IIa pretest SEM under 10x
Fig 77:	SEM photomicrograph of Group IIb pretest SEM under 10x
Fig 78:	SEM photomicrograph of Group IIa pretest SEM under 500x
Fig 79:	SEM photomicrograph of Group IIb pretest SEM under 500x
Fig 80:	SEM photomicrograph of Group Ia fractured alloy surface under 10x
Fig 81:	SEM photomicrograph of Group Ia fractured alloy surface under 250x
Fig 82:	SEM photomicrograph of Group Ia fractured alloy surface under 500x
Fig 83:	SEM photomicrograph of Group Ia fractured alloy surface under 1000x
Fig 84:	SEM photomicrograph of Group Ia fractured acrylic surface under 10x
Fig 85:	SEM photomicrograph of Group Ia fractured acrylic surface under 250x
Fig 86:	SEM photomicrograph of Group Ia fractured acrylic surface under 500x
Fig 87:	SEM photomicrograph of Group Ia fractured acrylic surface under 1000x
Fig 88:	SEM photomicrograph of Group Ib fractured alloy surface under 10x
Fig 89:	SEM photomicrograph of Group Ib fractured alloy surface under 250x
Fig 90:	SEM photomicrograph of Group Ib fractured alloy surface under 500x
Fig 91:	SEM photomicrograph of Group Ib fractured alloy surface under 1000x

- Fig 92: SEM photomicrograph of Group Ib fractured acrylic surface under 10x
- Fig 93: SEM photomicrograph of Group Ib fractured acrylic surface under 250x
- Fig 94: SEM photomicrograph of Group Ib fractured acrylic surface under 500x
- Fig 95: SEM photomicrograph of Group Ib fractured acrylic surface under 1000x
- Fig 96: SEM photomicrograph of Group IIa fractured alloy surface under 10x
- Fig 97: SEM photomicrograph of Group IIa fractured alloy surface under 250x
- Fig 98: SEM photomicrograph of Group IIa fractured alloy surface under 500x
- Fig 99: SEM photomicrograph of Group IIa fractured alloy surface under 1000x
- Fig 100: SEM photomicrograph of Group IIa fractured acrylic surface under 10x
- Fig 101: SEM photomicrograph of Group IIa fractured acrylic surface under 250x
- Fig 102: SEM photomicrograph of Group IIa fractured acrylic surface under 500x
- Fig 103: SEM photomicrograph of Group IIa fractured acrylic surface under 1000x
- Fig 104: SEM photomicrograph of Group IIb fractured alloy surface under 10x
- Fig 105: SEM photomicrograph of Group IIb fractured alloy surface under 250x
- Fig 106: SEM photomicrograph of Group IIb fractured alloy surface under 500x
- Fig 107: SEM photomicrograph of Group IIb fractured alloy surface under 1000x
- Fig 108: SEM photomicrograph of Group IIb fractured acrylic surface under 10x
- Fig 109: SEM photomicrograph of Group IIb fractured acrylic surface under 250x
- Fig 110: SEM photomicrograph of Group IIb fractured acrylic surface under 500x
- Fig 111: SEM photomicrograph of Group IIb fractured acrylic surface under 1000x

INTRODUCTION

In removable prosthodontics, partial dentures are commonly fabricated with acrylic resin and metal alloys.^{18,48,32} The choice of alloy for the removable partial denture (RPD) framework is based upon criteria, such that, it should be non-toxic, non allergenic, corrosion resistant, easy to use, relatively inexpensive and have adequate strength^{2,6}.

Traditionally noble metal alloys were used for the fabrication of RPD frameworks. Base metal alloys were introduced as an alternative to noble alloys. Co-Cr alloys are the most common base metal alloy used for removable prosthesis that incorporates metal components. Co-Cr alloys are relatively inexpensive and are approximately twice as rigid as Au alloys, but may contain elements that cause sensitivity or allergic reactions in some patients. Additionally laboratory manipulation of these alloys is difficult.^{2,6,21} Recently, titanium and its alloys have been increasingly used in clinical practice for RPD frameworks. Despite drawbacks such as lengthy burn out, difficulties in machinability, casting, polishing, inferior flexibility and higher initial costs, advantages such as its excellent corrosion resistance, biocompatibility, strength and ductility, render titanium as an ideal biomaterial for removable partial denture.^{21,24,28,37,38,41,45}

Heat polymerized acrylic resin is generally utilized for attaching artificial acrylic teeth to cast partial frameworks.^{2,18,48} Acrylic resin has many

advantages which include, its similarity in appearance to oral tissues and its ease of manipulation, but it also has disadvantages such as poor mechanical properties and residual monomer that may cause allergic and hypersensitive reactions.^{2,6}

Durability of the removable partial denture is dependent on the strong adhesion between the metal framework and acrylic resin.^{4,18,21} However the junction between the metal alloy and acrylic resin is an area of clinical concern. Microleakage at this junction may result in resin discolouration, fluid percolation, microbial proliferation and deterioration of contact between the metal alloy and acrylic resin. RPD failures are usually linked to this interface.^{34,44}

In the oral environment, the bond between the acrylic resin and metal must withstand continual exposure to occlusal forces, saliva and temperature variations occurring during ingestion of hot and cold food and drink. The difference in the coefficient of thermal expansion between the metal and acrylic resin is considerable. The lack of adhesion and the difference in the coefficient of thermal expansion together places severe demands on the metal/acrylic interface.^{18,32,44} The absence of bonding between the unprepared metal alloy and acrylic resin interface is well documented.^{44,61} Various methods for alloy surface preparations have been suggested to achieve an improved bond.²⁹ Metal surface treatments have been classified as mechanical and chemical. Mechanical bonding relies on macromechanical design and

micromechanical treatment of the alloy. Chemical bonding may be interfacial or adhesive in nature.⁴⁴

The macromechanical retention for a denture base resin is usually provided by the framework design in the prosthesis by using beads, posts, bars, lattice and mesh.^{32,34,37,44,48,61} Previous studies have compared the various macromechanical retention designs. Although the open lattice design provided higher retention to the denture base resin, it was more susceptible to permanent deformation. The mesh design has been suggested as suitable for most situations with buccal and lingual reinforcement of mesh retention design.^{8,29} Hence this mesh design was incorporated as the macro-mechanical retention design in this study. The major disadvantage of macromechanical retention between the denture base resin and metal framework is poor marginal sealing which permits microleakage and its sequelae.^{32,34,37,44,48,61}

With a view to minimize these problems, micromechanical retention has been suggested. Micromechanical retention increases the surface area and enhances the wettability by increasing surface-free energy. Micromechanical retention includes electrolytic etching, gel (acid) etching and air abrasion.⁴⁴ The retentive strength of acrylic resin to acid-etched frameworks has also been reported as an alternative to mechanical retention.²⁹ Although, electrochemical etching and acid etching significantly improve in bond strength they are associated with expensive equipment, technique sensitivity and harmful chemicals. Studies have shown that air abrasion improves the bond strength,

by increasing the surface area.⁷ Studies have suggested that air abrasion as one of the mechanisms of consistently improving the bond strength without the above drawbacks.^{15,18,44} Hence air abrasion was chosen to provide micromechanical bond in this study.

Chemical bonding between the metal framework and the denture base resin is also important. Poor chemical bonding in this area is a significant problem, which often results in adhesive failure.^{4,6,37,44} Chemical bonding was developed as an alternative to etching systems.⁴⁴ Chemical bonding systems reduce the gap at the resin/metal interface thus minimizing microleakage. Kourtis classified chemical bonding systems into three main groups according to their mechanism of adhesion, namely, silica coating, tin plating and bonding agents with active acrylate monomers.²⁹

Silica coating procedures produce an intermediate layer containing silicon dioxide on the metal surface providing sufficient bonding to acrylic resin. Several studies have demonstrated that silica coated metal exhibited significantly higher bond strength than electro-etched metal.^{29,30,31,32} Available silica coating systems like Rocatec, Silicoater MD require expensive equipment and strong potentially corrosive chemicals.^{4,29} Tin plating is relatively easily performed with consistent results, although lower bond strengths have been reported for base metal alloy.⁴⁴ Adhesive primers containing functional methacrylate monomers have been successfully synthesized and used as primers for bonding acrylic resin to dental alloys.^{6,29}

The availability of adhesive primers that are capable of chemical bonding to dental base metal alloys has simplified the surface preparation procedure.²¹ The application of a 4-methacryloxyethyl trimellitate anhydride (4-META) has been recommended for bonding Co-Cr alloys.^{6,16,18,21,28} Recently primers containing 10- methacryloxydecyl dihydrogen phosphate (MDP) have been developed to enhance the bonding of resin to base metal alloys.^{6,18} The 6-(4-vinylbenzyl-n-propyl) amino-1,3,5-triazine-2,4-dithione (VBATDT) has been found to be an effective primer when used on noble metals.⁶ Recent studies have reported that a primer containing both MDP and VBATDT, is effective in achieving the improved bonding between the heat polymerized resin and base metal alloys such as Co-Cr alloy and cp titanium.^{6,18,21,28} Hence this adhesive primer was used for chemical bonding in this study.

Water storage and thermocycling influence the properties of the material used in the prosthesis thereby simulating one of the factors in the oral environment. Thermocycling procedures represent the various temperature changes to which the prosthesis subjected during use. The loss of bond strength due to water storage and thermocycling has been well documented.^{18,20,32,50}

Surface treatments produce alterations in the surface texture of the alloy. Alteration of surface profile may affect the contact surface area of the metal which is available for both mechanical and chemical bonding. Surface analysis quantitatively by 3-D surface profilometry and qualitatively by

scanning electron microscopy respectively, aids in better visualization of the treated surfaces and failure patterns. The possible influence of an increase in surface area subjected to air abrasion with different grit sizes as measured by 3-D surface profilometry, on the bond strength has been quoted in a study⁷. Other studies have employed pre and post testing SEM analyses to qualitatively assess the surface topography and understand the modes of failure.^{18,37,61} In these studies various grit sizes for air abrasion and chemical bonding systems, have been compared. Combined 3-D surface profilometric and scanning electron microscopic comparative analyses of air abraded alloy surfaces with alloy surfaces subjected to air abrasion followed by Alloy Primer application are sparse.

Many studies have evaluated the adhesion of composite veneering to titanium and its alloys with adhesive primers and have reported higher bond strength values as applicable to fixed prosthodontics. However studies evaluating the bond between Ti alloy and denture base resin as applicable in removable prosthodontics are relatively few.²¹ Also comparative studies on the bond strength of denture base resin to Co-Cr alloy and Ti-6Al-4V alloy are still fewer. In these studies, the alloy samples have a smooth, flat surface design subjected to different surface treatments.^{18,21,28,37} Aging and thermocycling parameters have not always been included in these study design. Studies which comparatively evaluate the shear bond strength between denture base resin to Co-Cr alloy and Ti-6Al-4V alloy samples incorporating a

mesh design subjected to different surface treatments followed by aging and thermocycling procedures prior to testing are lacking.

In light of the above considerations, the aim of the present in-vitro study was to comparatively evaluate the shear bond strength of heat polymerized acrylic resin to Co-Cr and Ti-6Al-4V alloys with two different surface treatments, namely, air abrasion and air abrasion followed by Alloy Primer application after being subjected to aging and thermocycling and correlated with quantitative 3-D surface texture analyses of treated alloy samples along with pre and post testing SEM analyses.

The objectives of the present study included the following:

1. To evaluate the shear bond strength of heat polymerized acrylic resin to Co-Cr alloy samples treated with two different surface treatments, namely, air abrasion and air abrasion followed by Alloy Primer application after aging and thermocycling.(Group Ia and Group Ib)
2. To evaluate the shear bond strength of heat polymerized acrylic resin to Ti-6Al-4V alloy samples treated with two different surface treatments, namely, air abrasion and air abrasion followed by Alloy Primer application after aging and thermocycling.(Group IIa and Group IIb)
3. To compare the shear bond strength values of heat polymerized acrylic resin to Co-Cr alloy samples treated with two different surface treatments after aging and thermocycling.(Group Ia with Group Ib)

4. To compare the shear bond strength values of heat polymerized acrylic resin to Ti-6Al-4V alloy samples treated with two different surface treatments after aging and thermocycling. (Group IIa with Group IIb)
5. To compare the shear bond strength values of heat polymerized acrylic resin to Co-Cr alloy and Ti-6Al-4V alloy samples treated with air abrasion after aging and thermocycling. (Group Ia with Group IIa)
6. To compare the shear bond strength values of heat polymerized acrylic resin to Co-Cr alloy and Ti-6Al-4V alloy samples treated with air abrasion followed by Alloy Primer application after aging and thermocycling. (Group Ib with Group IIb)
7. To quantitatively evaluate the surface texture of one representative test sample each of Co-Cr and Ti-6Al-4V alloys subjected to two different surface treatments respectively, prior to acrylisation by 3-D surface profilometry.
8. To qualitatively evaluate the surface topography of one representative test sample each of Co-Cr and Ti-6Al-4V alloys subjected to two different surface treatments respectively, prior to acrylisation by scanning electron microscopy (SEM analysis).
9. To qualitatively evaluate the mode of failure of the one representative acrylised and tested samples of the four test groups by scanning electron microscopy (SEM analysis).

REVIEW OF LITERATURE

Lamstein A et al (1956)²⁵ presented experimental evidence to confirm the existence of marginal seepage and percolation under acrylic resins of the gold acrylic resin veneer crowns, made with and without window perforation. They found that crowns with perforations exhibited more marginal seepage.

Dunny AJ, King GE et al (1975)¹³ tested the effect of nine acrylic retention designs on shear strength of acrylic resin attachment to the partial denture framework in anterior edentulous spaces. Framework designs that allowed a greater bulk of acrylic resin projecting through openings in retention design, offered strong retention.

Livaditis J et al (1982)²⁶ described a technique for the retentive mechanism for the resin bonded retainers and described about the development and clinical application of electrolytic etching process. They described a technique of etching the inner side of cast fixed partial denture which is bonded to acid etching enamel surface.

Crim GA, Swartz ML et al (1985)¹¹ compared the effectiveness of four thermocycling techniques with tracers. Two thermocycling systems with different dwell times were used. They found no significant difference among the four thermocycling techniques and all demonstrated leakage.

Tanaka T et al (1986)⁵¹ devised a method of treating the interior surface of the lingual metal wings for effectively bonding adhesive to Ni-Cr

and Co-Cr alloys. They concluded that sufficient bonding strength and adhesion was obtained for the Co-Cr alloy by merely sandblasting with alumina and ultrasonic wave polishing even after thermocycling.

Zurasky EL et al (1987)⁶¹ compared and concluded that the retentive bond strength of an acid etched base metal to acrylic resin was 3.5 times greater than that obtained with bead retention.

Brown DT et al (1987)⁸ compared the fatigue strength of acrylic retention designs including mesh, reinforced mesh design, lattice and smooth plate. They concluded that mesh retention as suitable for most situations and with buccal and lingual reinforcement of mesh design.

Yamauchi M et al (1988)⁵⁶ revealed some casting defects of pure titanium and follow-up observations of patients with these dentures. Casting in the mesh type wax pattern less than 0.35mm thick produced more incomplete form of mesh and suggested a minimum mesh thickness of 0.7mm.

Jacobson TE et al (1988)¹⁶ compared the bond strength of a conventional polymethylmethacrylate acrylic denture base with an acrylic resin containing 4-META to Co-Cr metal alloy by using various designs representative of clinical situations. They found higher bond strength between the 4-META resin and the alloy.

May KB et al (1993)³⁰ compared the shear bond strength between polymethylmethacrylate resin and titanium treated with 110µm alumina air

abrasive and with 110µm alumina air abrasive plus silicoating. They concluded that surface treatment of titanium treated with 110µm alumina air abrasive plus silane coating increased the bond strength of titanium to polymethylmethacrylate.

Barclay CW et al (1994)⁵ compared the tensile and shear bond strengths of two self-cure acrylic resins to cobalt-chromium alloy (Co-Cr) samples, prepared with six surface finishes. The strongest mean tensile bond strength was recorded between the 4-Meta incorporated acrylic resin and Silicoated cobalt-chromium alloy.

Kononen M et al (1995)²² published a clinical report of treating a partially edentulous patient, who was hypersensitive to other metals with a titanium cast partial denture with a two year follow up without complications. They concluded that titanium was a relatively newer and alternative material for removable partial denture frameworks.

May KB et al (1995)³¹ compared the shear bond strength between the polymethylmethacrylate and titanium treated with 110µm alumina air abrasive and the Rocatec system. The results of their study showed that Rocatec bonding material could withstand higher shear forces at the titanium-polymethylmethacrylate interface.

Nabdalung DP et al (1997)³⁴ compared the shear bond strength of a traditional denture base resin and three adhesive denture base resins to treated

nickel chromium alloy with four alloy surface pretreatments (sandblast, Met-etch, Rocatec with silane, Rocatec without silane). They concluded that with primer, the traditional resin, primed Rocatec-silane treated group had the highest bond strength than nonprimed groups. However use of primers for adhesive denture base resins significantly reduced their bond strengths.

Canay et al (1997)¹⁰ tested the effect of relining the 4-META adhesive resin onto a partial denture framework. While samples with adhesive exhibited significantly greater bond strength than the others, samples without adhesive were ranked in the order mesh, ring-shaped and flat planes with regard to shear bond strength.

Mudford L et al (1997)³² investigated the fatigue failure between the titanium alloy and heat cure PMMA acrylic resin. They compared two different surface treatments (sandblasting with 250µm aluminium oxide and silicoater system) of the alloy and two different acrylic resins, after thermocycling. They concluded that samples subjected to silicoating system showed highest fatigue strength than samples subjected to sandblasting alone.

Nabdalung DP et al (1998)³⁵ studied the effectiveness of adhesive systems for Co-Cr alloys. They compared two surface pretreatments (sandblasted, sandblasted-electrochemically etched) and three adhesive primers. The tensile bond strength of primed specimens showed significantly higher bond strength than unprimed specimens.

Zinelis S et al (2000)⁶⁰ evaluated the effect of pressure of helium, argon, krypton and xenon on the porosity, microstructure and mechanical properties of commercially pure titanium castings and concluded that porosity and mechanical properties are dependent on the gas type, whereas the microstructure remained unaffected.

Ohkubo C et al (2000)³⁷ examined the shear bond strengths of denture base resin to pure titanium, Ti-6Al-4V and Co-Cr alloy using various adhesive primers after aging and thermocycling. The cast specimens were grit blasted with 50µm and treated with five different adhesive primers (Metal primer II(MP), Cesead opaque primer(OP), Experimental primer(EP), Meta Base(MB), Siloc bonding system(SI)). All 5 primers significantly improved the shear bond strengths of a denture base resin to all three alloys.

Sharp B et al (2000)⁴⁴ determined the effects of various metal surface treatments protocols on microleakage between the Ni-Cr-Be alloy used in RPD and acrylic resin. Test specimens were surface treated with air abrasion, tin plating and silanation individually and in all combinations. Specimens were acrylised, aged and thermocycled before being immersed in sodium fluorescein dye for 24 hours. Microleakage was assessed. Air abrasion alone and in combination with tin plating and silanation resulted in a significant reduction in microleakage.

Kuphasuk C et al (2001)²⁴ compared the corrosion behavior of six titanium materials through electrochemical polarization in 37°C ringers

solution. The corrosion rate for each alloy was compared with that of other alloys. Cp Ti and Ti alloys were more resistant to corrosion than NiTi.

Taira Y et al (2003)⁵⁵ evaluated the adhesive performance of metal conditioners used for bonding between auto-polymerizing resins and Ti-6Al-7Nb alloy. Alloy samples were air-abraded with alumina, and bonded with 24 combinations of eight metal conditioners including Alloy Primer and acrylised with three self cure resins. Shear bond strengths were determined both before and after thermocycling. They recommended the use of Alloy Primer or similar primers (COP and MP11) before acrylisation.

Eliopoulos D et al (2004)¹⁴ evaluated the porosity of cpTi castings produced with different casting machines, namely, inert gas arc melting casting machine, centrifugal casting machine and in the high frequency induction melting gas pressure casting machine. They concluded that the type of casting machine does not significantly influence the internal porosity.

Takahashi S et al (2005)⁴⁷ evaluated the shear bond strength and leakage of adhesive and nonadhesive PMMA to Ti-6Al-Nb alloy and cobalt – chromium alloy primed with three adhesive primers after thermocycling. The bond strength was significantly reduced by thermocycling and the adhesive systems improved the bond strength of Ti-6Al-Nb and cobalt –chromium alloys.

Shimizu H et al (2006)⁴⁶ investigated the shear bond strengths of an autopolymerizing denture base resin to cast Ti-6Al-7Nb and Co-Cr alloys using three metal primers including Alloy Primer after air-abrasion with 50µm alumina with and without thermocycling. All three metal conditioners significantly improved shear bond strengths of the autopolymerizing denture base resin to both Ti-6Al-7Nb and Co-Cr, with a considerable decrease in the bond strength of Ti-6Al-7Nb than that of the Co-Cr after thermocycling.

Barclay CW et al (2007)⁷ evaluated the importance of grit size of alumina in the preparation of Co-Cr alloy and to determine the effect of tensile bond strength of four different acrylic resins to the Co-Cr alloy. Co-Cr alloy specimens were air abraded with four different grit sizes of alumina particles, namely, 50µm, 110µm, 250µm, mixture of 180-330µm and then acrylised with four types of acrylic resins (self-cured 4-META resin, heat cured 4-META resin, self-cured resin, heat cured resin). Specimens were aged or thermocycled and tested for tensile bond strength. One surface treated sample from each group was subjected to 3-D contact surface profilometry for evaluating the available contact area for bonding. SEM analyses were carried out on the surface treated alloy sample to assess the surface topography and also on the debonded specimens to evaluate the mode of failure. They concluded that grit blasted Co-Cr alloy with varying alumina particles created an altered surface profile. They concluded that the type of acrylic resin rather than grit size used significantly affected the bond strength.

Okhubo C et al (2008)³⁸ described the laboratory conditions needed for fabricating titanium frameworks and the present status of titanium removable prostheses. They stated that there was a gradual increase in using titanium for cast RPD frameworks. In their opinion, the laboratory drawbacks still remained, such as the lengthy burn-out, inferior castability and machinability, reaction layer formed on the cast surface, difficulty of polishing, and high initial costs. However, titanium RPD frameworks have never been reported to fail catastrophically. They recommended titanium as protection against metal allergy, particularly for cast removable prostheses.

Rodrigues RCS et al (2009)³⁹ reviewed the applications of titanium and its status in prosthodontics. They described titanium and its alloys to have lightweight, high strength to weight ratio, low modulus of elasticity and excellent corrosion resistance and biocompatibility.

Banerjee S et al (2009)⁴ compared the tensile bond strength between the cobalt-chromium alloy and nickel-chromium alloys and autopolymerised acrylic resin using three primers containing different functional monomers and two processing techniques. They found that metal primer with MRB increased the bond strength of autopolymerized repair acrylic resin to base metal alloys.

Kim SS et al (2009)²¹ evaluated the shear bond strength of a heat cure denture base resin to commercially pure titanium , Ti-6Al-4V alloy and Co-Cr alloy using two adhesive primers (Alloy Primer, MR Bond). Alloy primer

containing the phosphoric monomer (MDP) improved the bonding between the heat cure acrylic resin to all alloys than a MR bond.

Ahmed A et al (2009)¹ tested the shear strength and type of failure between the lattice and mesh minor connectors with cold-, thermopress-, light-, and heat-cured acrylic resin bases. The mode of failure between the acrylic resin base and the minor connector differed for different types of acrylic resin and for different types of minor connectors. They concluded that for the mesh type of minor connector, the mode of failure in all acrylic resin types was adhesive, but with the lattice type, mode of failures included both adhesive and cohesive failure.

Van meerbeek B et al (2009)⁵³ reviewed the literature with regard to the different laboratory bond strength test results along with a review on clinical effectiveness of adhesives and potential relationship between laboratory bond strength data and clinical outcomes. They recommended measuring the immediate and aged bond strengths to predict the clinical effectiveness.

Ishii T et al (2009)¹⁵ examined the effect of alumina air abrasion with 50-70 μ m under different pressures on bonding between an acrylic resin and silver palladium and titanium alloys subjected to thermocycling. Air abrasion with an air pressure of 0.6 Mpa was effective in enhancing retentive characteristics of the acrylic resin joined to the alloys.

Rodrigues RCS et al (2010)⁴¹ compared the occurrence of porosities and retentive force of cp titanium and Co-Cr removable partial denture circumferential clasps cast by induction/centrifugation and plasma/vacuum pressure. cpTi specimens cast by latter method showed more porosities than those cast using the former. This was not relevant for Co-Cr alloy castings.

Lim HP et al (2010)²⁸ compared the shear bond strength and failure types of a heat cure resin to cp Ti, Ti-6Al-4V alloy and Co-Cr alloy. Test samples were either air abraded with 250µm alumina or air abraded followed by application of alloy primer. Without metal conditioner, only adhesive failure was observed and with metal conditioner a mixed failure was observed. Conditioner containing VBATDT had a significantly positive effect on the bond between the PMMA denture base resin and the tested alloys.

Bulbul M et al (2010)⁶ evaluated the effect of metal primers on shear bond strength of acrylic resin to different types of metals. Specimens were cast in a Ti, Co-Cr and Au-Ag-Pt alloys and were air abraded with alumina particles with varying grit sizes. Specimens of each alloy were divided to receive one of the acrylic resins (heat polymerized, autopolymerised, microwave polymerized). The specimens were divided into four groups received one of the three primers (Metal primer, Alloy primer, Meta fast). All samples were aged and then thermocycled. They concluded that Shear bond strengths varied according to the metal primer, metal type and acrylic resin used. Metal primers promoted a significant increase in the adhesive bonding of

acrylic resins to metal alloys. Alloy primer demonstrated the highest shear bond strength among all primers.

Lee G et al (2010)²⁹ tested the force necessary to separate acrylic resin bases from test frameworks using primed and unprimed different acrylic retention designs (smooth metal plate, metal plate with bead retention, lattice retention and mesh retention). A significantly increased force was necessary to separate the acrylic from each design of primed test specimen compared with unprimed specimens of the same design. Primed mesh retention had significantly greater separation force than the primed lattice and smooth metal plate.

Kawaguchi T et al (2011)¹⁸ evaluated the effect of three priming agents and one silica coating system on the bond durability between two cpTi and Co-Cr alloys and a heat polymerized denture base resin and samples subjected to thermocycling. Alloy specimens were prepared and divided into five groups, 1) air abraded with 50µm alumina 2) Rocatec silica coating system 3) air abraded followed by Epicord Opaque primer 4) air abraded followed by Super bond application and 5) air abraded with alloy primer application. SEM images were taken to observe the surface topography of the samples surface treated with air abrasion and Rocatec silica coating system. The Alloy Primer group showed the highest bond strength of a heat-polymerized resin to both CP Ti and Co-Cr alloy before and after thermocycling.

Yilmuz A et al (2011)⁵⁷ compared the shear bond strength between the acrylic resin and Co-Cr alloy using a metal primer, Nd:YAG laser irradiation or both to the sandblasted surface of the alloy. Bond strength significantly increased by applying metal primer on to the laser irradiated surface.

MATERIALS AND METHODS

The present in-vitro study was conducted to comparatively evaluate the shear bond strength of heat polymerized acrylic resin to Co-Cr and Ti-6Al-4V alloys with two different surface treatments after being subjected to aging and thermocycling and correlated with quantitative 3-D surface texture analyses of treated alloy samples along with pre and post testing SEM analyses.

The following materials and equipment's were used for the study:

MATERIALS EMPLOYED:

- ❖ Custom made mold (Fig.1) (Fig.2a-e)
- ❖ Petroleum jelly (Teypal Industries Ltd, Chennai) (Fig.3)
- ❖ Pattern resin (GC corporation, Tokyo) (Fig.4)
- ❖ Preformed wax pattern (Bego, Germany) (Fig.5b)
- ❖ Inlay wax (GC Corporation, Germany) (Fig.5a)
- ❖ Sprue wax (Bego, Germany) (Fig.6)
- ❖ Surfactant spray (Aurofilm, Bego, Germany) (Fig.7)
- ❖ Silicon casting ring & crucible former (Delta, Delta labs, India) (Fig.8)
- ❖ Phosphate bonded investment (Wirovest, Bego, Germany) (Fig.9)
- ❖ Alumina and Magnesia based investment (Rematitan plus, Dentaaurum, Germany) (Fig.10)
- ❖ Investment liquid (Begosol, Bego, Germany) (Fig.11)
- ❖ Co-Cr alloy (Wironit, Bego, Germany) (Fig.12)

- ❖ Ti-6Al-4V alloy (Smedent Co-Ltd, China) (Fig.13)
- ❖ Aluminium oxide powder for air abrasion 250µm,50µm (Delta, India) (Fig.14a,14b)
- ❖ Modeling wax (Hindustan dental products, Hyderabad, India) (Fig.15)
- ❖ Model Plaster (Ramraju Surgical Cotton Mills Limited, Perumalpatti,India) (Fig.16)
- ❖ Separating medium (DPI- ,Mumbai, India) (Fig.17b)
- ❖ Heat cure acrylic resin (DPI-Heat cure polymer and monomer, Mumbai,India) (Fig.17a)
- ❖ Alloy primer (Kuraray Co Ltd, Tokyo, Japan) (Fig.18)
- ❖ Separating discs(L.M abrasives, Italy) (Fig.19a)
- ❖ Rubber polishing wheel (L.M abrasives, Italy) (Fig.19b)
- ❖ Wax solvent (Acrolyn, India) (Fig 20)
- ❖ Sandpaper (Jawan brand, India) (Fig.21a)
- ❖ Pumice (Delta, India) (Fig.21b)
- ❖ Distilled water (Diet, Pondichery, India) (Fig.22)

INSTRUMENTS AND EQUIPMENTS EMPLOYED:

- ❖ PKT instrument (Dispodent, India) (Fig.23)
- ❖ Stainless steel metal scale(Elom, India) (Fig.24a)
- ❖ Wax caliper (TDI, USA) (Fig.24b)
- ❖ Metal caliper (TDI, USA) (Fig.24c)
- ❖ Porcelain cup (Marvel, China) (Fig.25a)

- ❖ Measuring jar (Prolab, Chennai) (Fig.25b)
- ❖ Wax knife, Wax carver and Stainless steel spatula (Fig.26a, b & c)
- ❖ Bowl and Spatula (Classic, India) (Fig.27)
- ❖ Metal trimmers (Edenta, Switzerland) (Fig.28a)
- ❖ Acrylic trimmers (Shofu, Japan) (Fig.28b)
- ❖ Sandpaper mandrel (Sirag Dental Co., Chennai, India) (Fig.28c)
- ❖ Denture flask and dental clamp (Jabbar, India) (Fig.29)
- ❖ Vacuum power mixer (The Continental, Whipmix, Kentucky, USA)
(Fig.30)
- ❖ Burnout furnace (SUNBIM, India) (Fig.31)
- ❖ Crucible (Silicast, Furnace, Bego, Germany) (Fig.32)
- ❖ Induction Casting machine (FORNAX, Bego, Germany) (Fig.33)
- ❖ Casting Machine (NeutrodynEASYTiHD, India) (Fig.34)
- ❖ Sand Blaster (Ideal Blaster, Delta labs, Delta, Chennai) (Fig.35)
- ❖ Alloy grinder (Whipmix, USA) (Fig.36)
- ❖ Dental lathe (Suguna dental lathe, Suguna industries, Coimbatore,
India) (Fig.37)
- ❖ Acrylizer (Confident dental equipments limited) (Fig.38)
- ❖ Steam cleanser (OMEC, MUGGIO, MICANO, Italy) (Fig.39)
- ❖ Plastic containers (Isoplast, Approx Industries, India) (Fig.40)
- ❖ Incubator (Narang industries ltd, New Delhi) (Fig.41)
- ❖ Thermocycler (Haake, Willytec, Germany) (Fig.42)

- ❖ Universal testing machine (INSTRON, Lloyd instruments, UK) (Fig.43)
- ❖ Surface Profilometer (TalysurfCCI, Ametek, UK) (Fig.44)
- ❖ Scanning Electron microscope (SA400N,Canada) (Fig.45)

Description of the custom made mold:

In this study, a custom made stainless steel mold, (Fig.1a) (Fig.2) was fabricated to aid in standardizing the dimensions of test sample patterns. It consisted of five separate parts. A heavy base, of dimensions 21cm x 12 cm x 2cm was fabricated (Fig.1b). Template 1 was fabricated to seat over the base. It had twelve, 1cm x 1cm square projections on top, each separated by 1cm (Fig.1d). Template 2 was fabricated to seat over the template 1. It had twelve square slots of dimensions 1.5cm x 1.5cm square with 1.6mm thickness corresponding to the twelve projections of the template 1 (Fig.1e). Template 3 was fabricated with similar twelve projections to match the design of the template 1 (Fig.1f). When templates 1, 2 and 3 were positioned sequentially one above the other on the base, the twelve projections of template 1 and template 3 contacted each other through the corresponding twelve slots of template 2. The mold space created was such that a square pattern of 1cm x 1cm and 1.6mm thickness with a space in the centre of dimensions 8mm x 8mm could be obtained. This space was meant for incorporating the mesh retention design in the samples. A heavy lid of similar dimensions as the base

was fabricated to fit over the entire assembly and to aid in executing uniform pressure over the sample patterns (Fig.1c).

Description of Alloy Primer:

Alloy Primer (Kuraray Co Ltd, Tokyo, Japan) (Fig.18) was used in the present study for chemical surface treatment of the alloy samples. It contains functional methacrylate monomers, namely, 6-(4-vinylbenzyl-n-propyl) amino-1, 3, 5-triazine-2, 4-dithione (VBATDT) and 10-methacryloyloxydecyl dihydrogen phosphate (MDP). Due to the VBATDT and MDP, Alloy Primer enhances the bond strength to both precious and also non precious metals. It is applied to the metal adherend surface with a suitable applicator tip and the surface treatment is completed. According to the manufacturer, a single coat or at the most two such coats are sufficient. Mechanism of adhesion for non precious metals – Phosphoric acid group of MDP bonds chemically to the non precious atoms, while the double bonds on the other end of the molecule copolymerize with the resin monomers.

Description of the Thermocycler:

In this study, thermocycler (Haake, Willytec, Germany) (Fig.42) was used for thermocycling the test samples to simulate the temperature changes in the oral cavity. It consists of two water baths, each maintained at two different temperatures. Bath one has temperature variation from 25°C to 100°C and bath two has temperature variation from -5°C to 100°C. It has period times

adjustable via display from 0-9999 cycles. It has automatic refills for the baths to compensate evaporation during the long duration test. It has an auto start capability. Bath two is connected to a cooling device. The two baths are connected by a rolling unit with an open sample container in the centre for holding the test samples. **Principle of operation** – The open sample container with the test samples is immersed cyclically in baths of warm and cold water. Simulation of exposure of samples to various temperatures is effected thereby, and the resulting wide temperature fluctuations can reveal bond durability of the samples.

Description of the Universal testing machine:

The table top, universal testing machine was used to test for shear bond strength of the test samples used in this study (Instron, Lloyd instruments, UK) (Fig.43). It consists of a lower chamber, upper chamber, a display board to display the amount of force needed to fracture the samples and a computer. The upper member is attached to the lower with the help of two horizontal bars, which also encloses the hydraulic pressure machine attached to upper member. The lower portion has a bench vice test specimen fixture to hold the test specimen. The upper member has a Levis grip on which a monobeveled chisel blade can be attached. The whole unit is attached to the computer for recording and converting as required.

Description of the 3-D Surface Profilometer:

In the present study, the surface texture of the test samples was analyzed quantitatively using a 3-D Surface Profilometer (TalysurfCCI, Ametek, UK) (Fig.44). In the present study a non-contact optical 3-D Surface Profilometer was used to measure the 3-D surface texture. It is an advanced type of measurement interferometer. The 3D Non-Contact Profilometer is designed with leading edge optical lens using superior green light axial chromatism. Nano through macro range is obtained during measurement on a wider range of geometries and materials. 3D Non-Contact Profilometer optical lens have zero influence from sample reflectivity, variations require no sample preparation and have advanced ability to measure high surface angles. It can easily measure any material which is transparent, opaque, specular, diffusive, polished, rough etc. Unlike other optical measurement techniques, large surface areas can be precisely measured without any image stitching. From this, 3-D and advanced 3-D images can be viewed as well as average mean surface roughness (Ra) value calculated.

Description of the Scanning Electron microscope:

In the present study, the surface of the test samples were analyzed qualitatively using a Scanning Electron Microscope (SA400N, Canada) (Fig.45). Scanning Electron Microscope uses a beam of highly energetic electrons to examine objects on a very fine scale. They can reveal the fine structure of variety of materials. SEM uses a scanned beam rather than a fixed

beam. It is used primarily for the examination of thick samples. The specimens to be magnified may have some conductivity and may get charged up. Hence they are coated with a platinum layer to prevent the charging up and in order to increase the secondary emissions. Additional sputter coating with gold produces high contrast and resolution. It also increases the signal/noise ratio of the coated samples. The incident electron probe scans the sample surface and the signals produced are used to modulate the intensity of a synchronously scanned beam on a CRT screen. The electrons which are back scattered from the specimen are collected to provide (i) topographical information if low energy secondary electrons are collected (ii) atomic number and reorientation information if the higher energy, back scattered electrons are used, or if the leakage current to the earth is used. The magnification is given immediately by the ratio of the CRT scan size to the specimen scan size.

METHODOLOGY:

- I. Preparation of the alloy samples:**
 - a. Preparation of the Co-Cr alloy samples
 - b. Preparation of the Ti -6Al-4V alloy samples
- II. Grouping of the samples**
- III. Acrylization to the surface treated alloy samples**
- IV. Aging and thermocycling of the samples**
- V. Shear bond strength testing of the samples**
- VI. Quantitative analyses of surface treated alloy samples by 3-D non-contact surface profilometry**
- VII. Qualitative analyses of surface treated alloy samples and mode of failure by scanning electron microcopy.**

I. Preparation of the alloy samples:

a. Preparation of the Co-Cr alloy samples: The Co-Cr alloy samples were obtained in the following manner:

1. Pattern fabrication of Co-Cr alloy samples
2. Investment procedure of the patterns
3. Burnout of patterns and casting procedures
4. Finishing of Co-Cr alloy samples

1. Pattern fabrication of Co-Cr alloy samples:

Twenty two sample patterns of size 1cm x 1cm x 1.6mm with a space in the centre of dimensions 8mm x 8mm x 1.6mm were obtained with pattern resin, (GC corporation, Tokyo) (Fig.4) from the custom made mold (Figs.1 & 2). A preformed mesh pattern (Bego, Germany) (Fig.5b) of 1cm thickness was cut to 8mm x 8mm to fit the space in the centre of each pattern and secured using inlay wax (GC corporation, Germany) (Fig.5a) using PKT instrument (Dispodent, India) (Fig.23). Since the thickness of the mesh area was less than the thickness of the resin pattern, it resulted in a stepped appearance (Fig.46a-e). Each pattern dimension was checked for accuracy using metal scale (Elom,India) (Fig.24a) and wax caliper (TDI, USA) (Fig.24b). Sprues (Bego, Germany) (Fig.6) of 2.5mm diameter and 13mm length were attached to the patterns and to the crucible former (Delta, Delta

Labs, India) (Fig.47) at the other end. The patterns were sprayed with surfactant spray (Aurofilm, Bego, Germany) (Fig.7) to improve their wettability.

2. Investment procedure of the patterns:

Suitable size of the silicon casting ring (Delta,Delta Labs,India) (Fig.8) was selected and positioned on the crucible former around the prepared patterns. The patterns were invested with Phosphate bonded investment (Wirovest, Bego, Germany) (Fig.9) using the manufacturer's instructions. Powder and liquid in the recommended ratio was hand mixed for 15 seconds until a homogenous mix was obtained and then vacuum mixed for 120 seconds in a vacuum power mixer (The Continental, Whipmix, Kentucky, USA) (Fig.30). The mixed investment material was hand-painted on each pattern using a brush and then slowly poured into silicast ring until the ring was completely filled and allowed to set for 60 minutes. Since the ringless casting procedure was adopted in this study, the silicon casting ring was removed after the investment material had set (Fig.48).

3. Burn out of patterns and casting procedures:

The set investment mold was placed in the burnout furnace (SUNBIM, India) (Fig.31) at room temperature. Investment mold was allowed to heat continuously till 950°C at the rate of 8°C per minute and held for 30 minutes at 950°C. Casting procedure was performed immediately subsequent to burnout to prevent heat loss from the mold. After burn out, the investment mold was

taken out of the furnace and placed in the casting machine. Casting was done in induction casting machine (FORNAX, Bego, Germany) (Fig.33). Co-Cr alloy ingots were (Wironit, Bego, Germany) (Fig.12) was heated sufficiently till they melted completely and the crucible (Silicast, Bego, Germany) (Fig.32) was released. Centrifugal force ensured completion of the casting procedure. Investment with cast was allowed to cool down to room temperature. Divestment was done to retrieve the castings (Fig.49).

4. Finishing of Co-Cr alloy samples:

Divested castings were grit blasted using alumina particles with a grit size of 250 μ m (Delta,India) (Fig.14a) to remove the adhering investment. Sprues were sectioned with separating discs (L.M Abrasives, Italy) (Fig.19a) attached to a disc mandrel (Shofu, Japan) (Fig.28a). The metal specimens were visually inspected for discrepancies. As per standard protocol, finishing of the alloy samples were carried out, using tungsten carbide trimmers (Fig. 28a) and rubber polishing wheels (L.M Abrasives ,Italy) (Fig.19b). A total of 22 Co-Cr alloy samples were thus obtained (Fig.50).

b. Preparation of the Ti-6Al-4V alloy samples: The Ti-6Al-4V alloy samples were obtained in the following manner:

1. Pattern fabrication of Ti-6Al-4V alloy samples
2. Investment procedure of the patterns
3. Burnout of patterns and casting procedures
4. Finishing of Ti-6Al-4V alloy samples

1. Pattern fabrication of Ti-6Al-4V alloy samples:

Twenty two sample patterns of similar dimensions and design, as described for obtaining the patterns for Co-Cr alloy samples were fabricated. Sprues of 2.5mm diameter and 13mm length were attached to the patterns and to the crucible former at the other end. The patterns were aligned vertically and sprued to a horizontal runner bar (Fig.51) since casting of Ti alloys is based on the flow of molten metal by gravity under vacuum. The patterns were sprayed with surfactant spray to improve the wettability.

2. Investment procedure of the patterns:

Suitable size of the silicon casting ring was selected and positioned on the crucible former around the prepared patterns. The patterns were then invested using silicate-and phosphate-free, magnesia and alumina-based investment (Rematitan plus, Dentaurem, Germany) (Fig.9) following the manufacturer's recommendations. Powder and liquid in the recommended ratio was hand mixed for 15 seconds until a homogenous mix was obtained and then vacuum mixed for 120 seconds in a vacuum power mixer. The mixed investment material was hand-painted on each pattern using a brush and then slowly poured into silicast ring until the ring was completely filled and allowed to set for 90 minutes. Since the ringless casting procedure was adopted in this study, the silicon casting ring was removed after the investment material had set.

3. Burn out of patterns and casting procedures:

The set investment mold was heated in the burnout furnace to 250°C with a heating rate of 5°C/min and held constant for 90 minutes. The temperature was then raised to 900°C with the same heating rate and held at 900°C for 30 minutes. Then the investment mold was cooled down slowly at a rate of 5°C/min to 430°C was held at that temperature for 30 minutes. When the burnout cycle was completed, the investment mold was placed into the Ti casting machine (NeutrodynEASYTiHD, India) (Fig.36). To avoid contamination, the casting machine was thoroughly cleaned before and in between subsequent castings. Upon starting of casting, the closed interconnected two chamber system of the casting machine allowed automatic melting and casting to take place under vacuum with inert argon gas under a pressure of 0.8 bar. After casting was completed, the casting rings were immediately quenched under tap water to suppress the reactivity of the molten Ti alloy with the atmosphere. Divestment was done to retrieve the castings.

4. Finishing of Ti-6Al-4V alloy samples:

Divested castings were subjected to similar finishing procedures as described previously for finishing of Co-Cr alloy samples. A total of 22 samples of Ti-6Al-4V alloy were thus obtained (Fig.52).

II. Grouping of the samples:

A total of 44 alloy samples were obtained of which, 22 samples were of Co-Cr alloy and 22 samples were of Ti-6Al-4V alloy. The Co-Cr alloy

samples were designated as Group I and the Ti-6Al-4V alloy samples were designated as Group II. The samples within the Groups I and II were further randomly and equally divided into Groups Ia and Ib and Groups IIa and IIb based on the following surface treatments:

Group Ia samples were subjected to air abrasion with 50 μ m alumina prior to acrylisation. **Group Ib** samples were subjected to air abrasion with 50 μ m alumina followed by Alloy Primer application prior to acrylisation. **Group IIa** samples were subjected to air abrasion with 50 μ m alumina prior to acrylisation. **Group IIb** samples were subjected to air abrasion with 50 μ m followed by Alloy Primer application prior to acrylisation.

One representative, surface treated alloy sample from each test group was randomly selected. These samples were subjected to quantitative surface texture analyses using 3-D non-contact surface profilometer and qualitative surface topography analyses using scanning electron microscopy, which will be described later. The remaining ten surface treated samples from each test group were acrylised and subjected to shear bond strength testing procedures.

III. Acrylization to the surface treated alloy samples:

1. Waxing of the alloy samples:

Ten alloy samples of each test group were waxed prior to acrylic resin processing using modeling wax (Hindustan dental products, Hyderabad, India) (Fig.15) and accomplished with a wax knife (Fig.26a). The wax up was

finished flush, with the alloy sample with a cylindrical projection of dimensions 3.5cm length and 6.5mm in diameter from the centre of the test sample (Fig.53 a, b & c). The purpose of the cylindrical extension was to provide a means for holding the sample during shear bond strength testing procedures.

2. Flasking procedure:

A two pour technique was followed for flasking the waxed up specimens. Type II dental plaster (Ramraju Surgical Cotton Mills Limited, Perumalpatti, India) (Fig.16) was mixed with water using a stainless steel straight spatula (Fig.26c) in a rubber bowl (Classic, India) (Fig.27) poured into the lubricated base portion of the denture flask (Jabbar, India) (Fig.29). The waxed up alloy samples were placed into the mix (Fig.54). The number of samples per denture flask was restricted to a maximum of eight to ensure adequate space between the samples. After the plaster had set, separating medium (DPI, Mumbai, India) (Fig.17b) was painted over the plaster surfaces, and the lubricated body of the flask was placed over the base. It was filled with a fresh mix of type II dental plaster and the lid was closed. The denture flask was tightened with a flask carrier and the excess plaster removed. The flasks were marked to aid in identification of test groups.

3. Dewaxing procedure:

The plaster was allowed to harden for 1 hour before the denture flask was placed in a boiling water bath. The flasks were placed in boiling water for 4 minutes. The flask was removed from the water and the appropriate segments of the flask were carefully separated in a vertical direction to avoid fracture of the invested plaster. The softened wax was flushed out from the surface of the mold with hot water. Wax solvent (Acrolyn, India) (Fig.20) and warm detergent solution were used to remove wax residues and oily films respectively. Finally the molds were flushed well with clean hot water. Both the halves of the flasks were placed on end for several minutes to allow the water to drain completely. The flasks were allowed to cool completely prior to packing. After dewaxing, the base of the denture flask carried the invested alloy samples and the body exhibited the cylindrical mold spaces for the acrylic resin (Fig.55).

4. Surface Treatment of the alloy samples:

After dewaxing procedures, the invested alloy samples of each group were subjected to different surface treatment protocols. The surface treatment procedures were carried out based on the grouping of the test samples. All samples of test groups Ia, Ib, IIa and IIb were air abraded with alumina particles with a grit size of 50 μm (Delta, Delta labs, India) (Fig.14b) using a sand blaster, with the nozzle positioned approximately 10mm from the sample surface for 15 seconds with a pressure of 0.6 Mpa. The air abraded surfaces

were cleaned with compressed air followed by steam cleansing using a steam cleanser (OMEC, MUCANO, Italy) (Fig.39). Alloy samples that moved during the above procedures were repositioned in the investment (Fig.56a).The sample surfaces were allowed to dry completely.

Further surface treatment was performed for groups Ib and IIb test samples, by the application of Alloy Primer (Kuraray Co Ltd, Tokyo, Japan) (Fig.18). A single coat of Alloy Primer was applied to the alloy surfaces using an applicator tip (Fig.56b) unidirectionally to avoid puddling and to obtain a uniform layer. It was allowed to air dry for 5 minutes as per the manufacturer's instructions. All surface treated samples were immediately packed with heat cure acrylic resin.

5. Packing procedure:

After accomplishing the surface treatment of the samples, a thin coating of separating medium was painted on the plaster surface. Care was taken to avoid contact with the surface treated alloy samples. Heat cure acrylic resin (DPI Polymer and monomer, Mumbai, India) (Fig.17a) was mixed in the porcelain cup (Marvel, China) (Fig.25a) with a powder/liquid ratio as per the manufacturer's instructions. The porcelain cup was closed with a lid until the mix reached the dough stage. Required quantity of acrylic resin dough was packed individually into each cylindrical mold space. The metal surfaces were not further wetted with monomer liquid before the resin dough was placed onto them. The two halves of the flask were closed and the flask was placed

under the bench press and tightened. The excess resin extruding from the flask was removed.

6. Polymerization procedure:

The packed denture flasks were bench cured for 60 minutes as per the manufacturer's instructions and the flasks were removed from the bench press. The flasks were tightened under their respective flask carriers and placed in the acryliser (Confident Dental Equipments Limited, India) (Fig.38) for resin polymerization. A curing cycle of 74°C for approximately 2 hours and then increasing the temperature of the water bath to 100°C and processing for 1 hour as per standard recommendations was followed for all packed test specimens.

7. Deflasking procedure:

After the completion of polymerization cycle, the flasks were removed from the water bath and bench cooled for 30 minutes and then kept under running tap water for 15 minutes. Following this, the deflasking of the specimens was done (Fig.57).

8. Finishing and polishing:

After the specimens were deflasked and excess plaster was removed. Acrylic burs (Shofu, Japan) (Fig.28b) were used to trim excess resin. Sandpapers of grit sizes of 100, 120, 180 and 220 (Jawan Brand, India) (Fig.21a) respectively were used to smoothen the surface, mounted on a sandpaper mandrel (Sirag Dental Co., India) (Fig.28c). Polishing was done

with pumice (Delta,India) (Fig.21b) using a rag wheel mounted on a dental lathe (Suguna Industries, Coimbatore, India) (Fig.37) (Fig.58). In this manner, a total of forty surface treated and acrylised samples of groups Ia, Ib, IIa and IIb were obtained (10 samples per group) (Fig.58). The test samples of each test group were stored in separate, labeled, plastic containers (Isoplast, Approx Ltd, India) (Fig.40) under distilled water (Diet, Pondichery, India) (Fig.22) (Fig.59a).

IV. Aging and thermocycling of the samples:

All the stored test samples of Groups Ia, Ib, IIa and IIb were subjected to aging. They were transferred to an incubator (Narang Industries Ltd, New Delhi, India) (Fig.41) and held at a temperature of 37°C for three days (Fig.59b).

After aging, all samples of Groups Ia, Ib, IIa and IIb were subjected to thermocycling for 500 cycles in a distilled water bath between 5°C and 55°C with a dwell time of 30 seconds and a dry time of 10 seconds using a thermocycling apparatus (Haake, Willytec, Germany) (Fig.42) (Fig.60). Upon completion of thermocycling, the specimens were stored in distilled water in their respective containers until they were subjected to shear bond strength testing.

V. Shear Bond Strength Testing of the Samples:

A total of forty samples (Groups Ia, Ib, IIa and IIb) were tested for shear bond strength in a universal testing machine (Instron, Lloyd Instruments,

UK) (Fig.43). Each test sample was fixed to the sample fixture at the bench vice of the machine with the monobevelled chisel blade placed adjacent to and directly to the bonding interface (Fig.61). Force was applied to the sample so that shear load was exerted adjacent and directly to the bonding interface at a cross head speed of 1mm/min until fracture occurred. Load deflection curves and ultimate load to failure were recorded automatically and displayed by the computer software of the testing machine. Shear bond force was recorded in Newton and shear bond strength (Mpa) was calculated through dividing the load (N) at which failure occurred by the bonding area (mm²)

$$\text{Bond strength (Mpa)} = \text{Load (N)} \div \text{surface area (mm}^2\text{)}$$

The basic and mean value data of shear bond strength obtained were tabulated individually for all four test groups (Group Ia, Ib, IIa and IIb) and was statistically analyzed. All statistical calculations were performed using Microsoft Excel (Microsoft, USA). The SPSS (SPSS for Windows 10.05, SPSS Software Corp. Munich, Germany) software package was used for statistical analysis. ‘T’-test was used to compare the mean values of each test groups and a P value < 0.05 was considered statistically significant. The tested samples (Fig.62) were retrieved and stored in their respective containers. One representative tested sample from each test group was randomly selected and qualitatively analyzed using SEM to assess the mode of failure.

VI. Quantitative analyses of surface treated alloy samples by 3-D surface profilometry:

Four samples, comprising of one representative treated alloy sample from each test group was subjected to 3-D surface profile scanning (TalysurfCCI, Ametek, UK) (Fig.44). 3-D surface roughness was measured using 3-D non-contact surface profilometer. The average surface roughness (Ra) values of each sample obtained. The magnification of the optical lens was 50x. Each sample was placed under the objective lens and photomicrographed at 50x magnification to obtain 3-D and advanced 3-D views using Advanced Aspherics Analysis Software.

VII. Qualitative analyses of surface treated alloy samples and mode of failure by scanning electron microscopy (SEM):

SEM Analysis was carried out on one representative surface treated alloy sample from each test group and also on one randomly selected sample from each test group after shear bond strength testing using a Scanning Electron Microscope (SA400N, Canada) (Fig.45).The samples were secured into Cu stubs with a double adhesive tape and coated with a layer of gold using gold sputtering system (Fig.63). Coated samples were examined under SEM to qualitatively assess the surface topography of surface treated samples at 10x and 500x magnifications. The mode of failure of tested samples was assessed at 10x, 250x, 500x and 1000x magnifications.

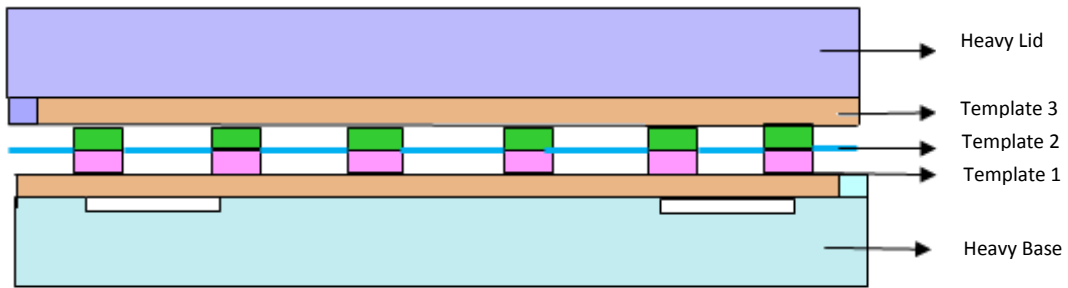


Fig.1a: Line diagram showing assembled custom made mold

Fig.1b-f: Line diagram of individual custom made mold parts

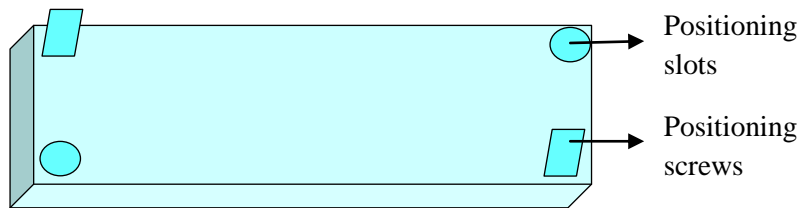


Fig.1b: Heavy base



Fig.1c: Heavy lid

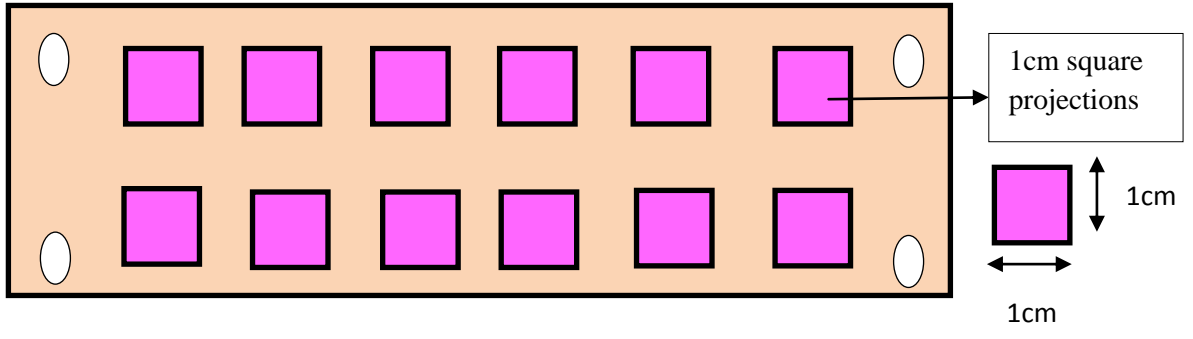


Fig.1d: Template 1

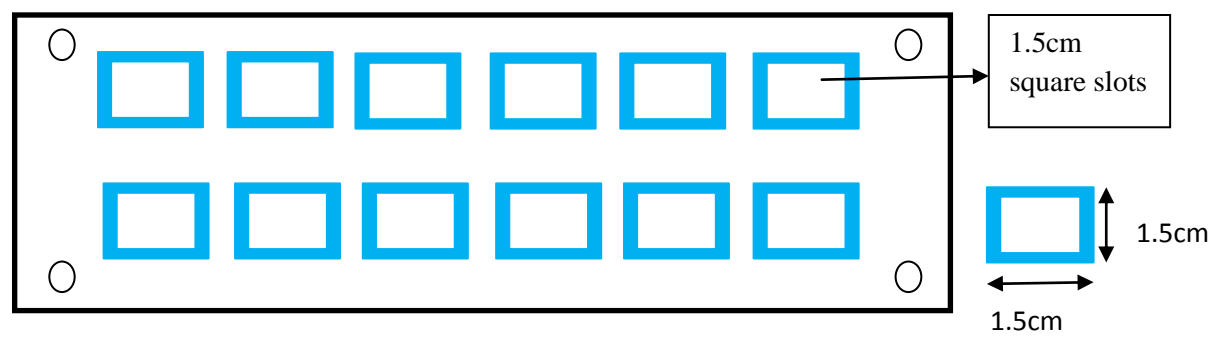


Fig.1e: Template 2

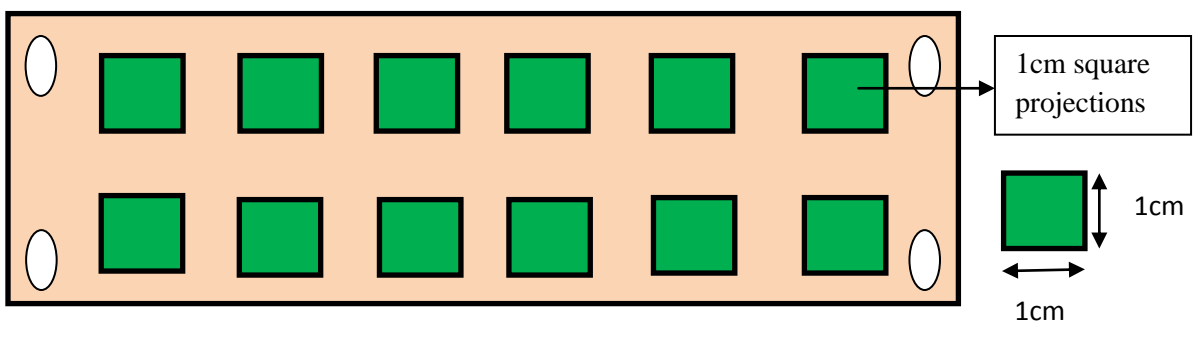


Fig.1f: Template 3

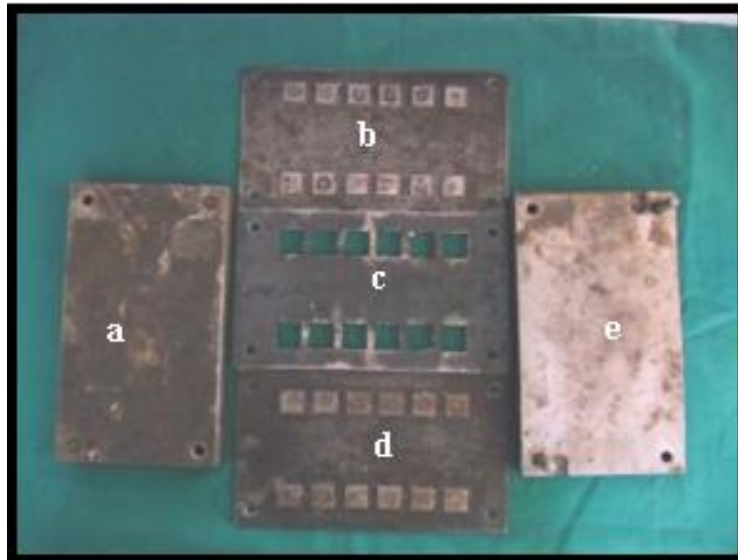


Fig.2a: Heavy base, 2b: Template1, 2c: Template2, 2d:Template 3, 2e: Heavy lid



Fig.3: Petroleum jelly



Fig.4: Pattern resin

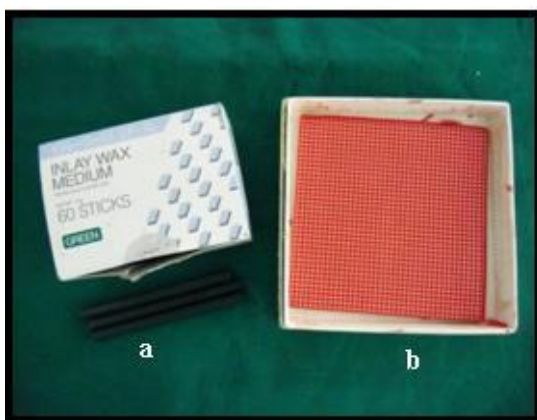


Fig.5a:Inlay wax,5b:Preformed mesh pattern



Fig.6: Sprue wax



Fig.7:Surfactant Spray



Fig.8: Casting ring



Fig.9: Phosphate bonded investment



Fig.10: Alumina and Magnesia based investment



Fig.11: Investment liquid



Fig.12: Co-Cr alloy



Fig.13: Ti-6Al-4V alloy



Fig.14a: Aluminium Oxide Powder 250 μ m
Fig.14b: Aluminium Oxide Powder 50 μ m

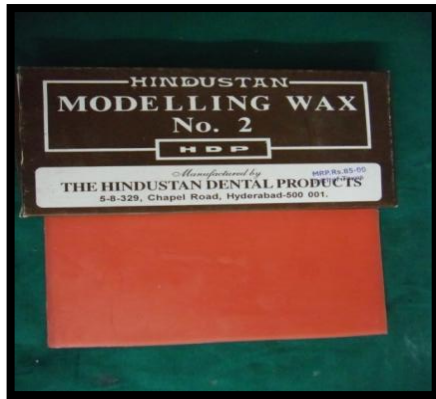


Fig.15 Modelling Wax



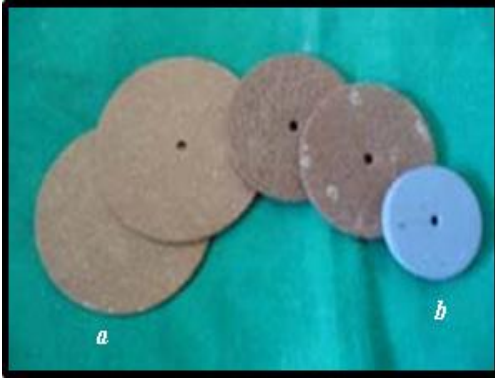
Fig.16 Model plaster



Fig.17a: Separating medium
17b: Heat cure polymer and monomer



Fig.18. Alloy primer



**Fig.19a: Separating discs,
19b: Rubber polishing wheel**



Fig.20: Wax solvent

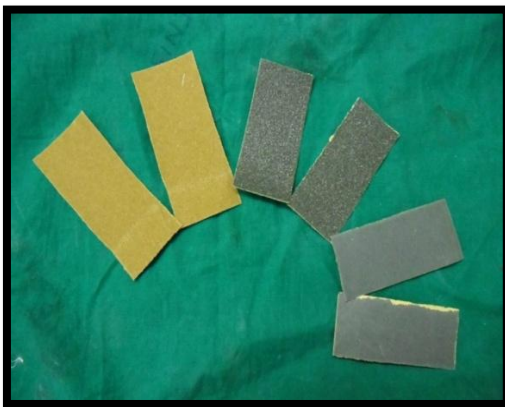


Fig 21a. Sandpaper of different grit sizes



Fig.21b: Pumice



Fig.22: Distilled water



Fig.23: PKT instrument



**Fig.24a: Stainless steel metal scale,
24b: Wax caliper, 24c: Metal caliper**



**Fig.25a: Porcelain cup
25b: Measuring jar**

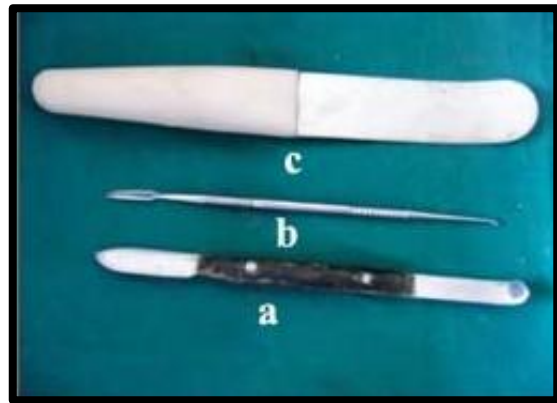


**Fig.26a: Wax Knife, 26b: Wax carver,
26c: Stainless steel spatula**



Fig.27: Rubber bowl



**Fig.28a: Metal Trimmers and Mandrel
28b: Acrylic Trimmers,
28c: Sand Paper Mandrel**



Fig.29: Denture flask



Fig.30: Vacuum power mixer



Fig.31: Burnout furnace



Fig.32: Crucible



Fig.33: Induction casting machine



Fig.34: Casting machine for Ti



Fig.35: Sandblaster



Fig.36: Alloy grinder



Fig.37: Dental lathe



Fig.38: Acryliser



Fig.39: Steam cleanser



Fig.40: Plastic Containers



Fig.41: Incubator



Fig.42: Thermocycler



Fig.43: Universal Testing Machine

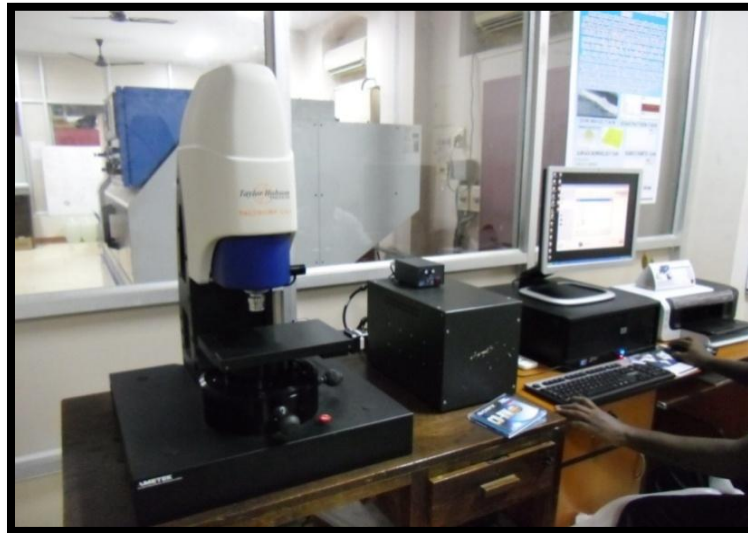


Fig.44: Surface Profilometer



Fig.45: Scanning Electron Microscope

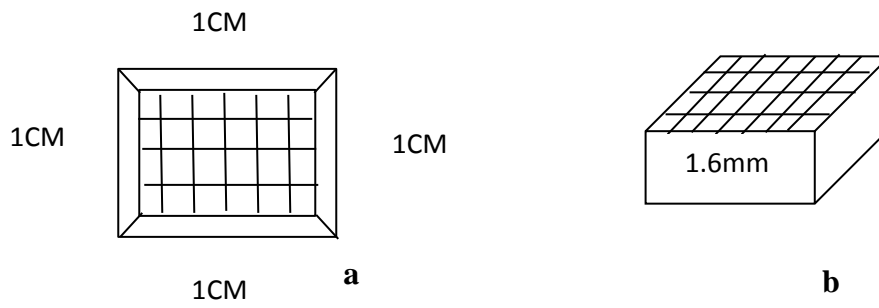


Fig.46a & b: Schematic diagram showing sample pattern dimensions.

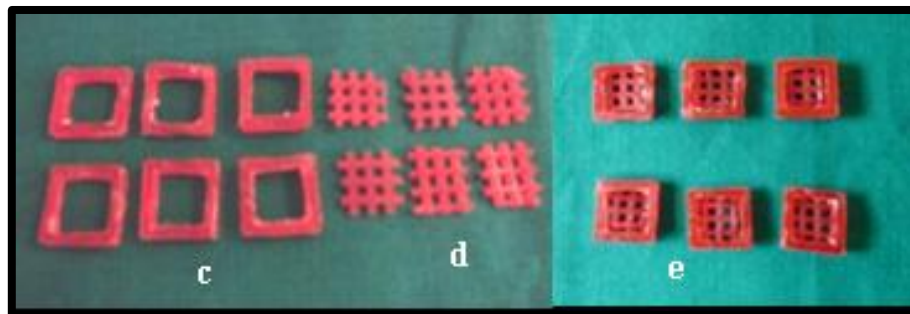


Fig.46c: Patterns with a space in the centre, 46d: Preformed mesh patterns, 46e: Finished sample patterns

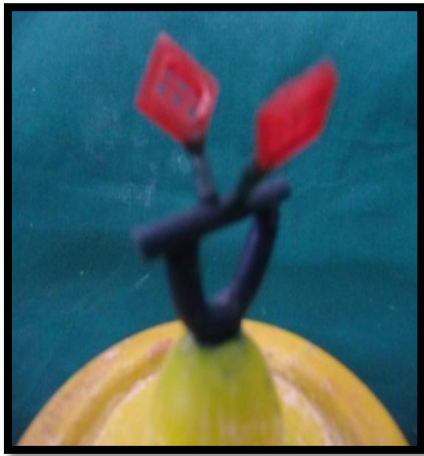


Fig.47: Sprues attached to the patterns and to the crucible former



Fig 48. Investment mold



Fig 49. Retrieved casting



Fig.50: Finished Co-Cr alloy samples



Fig.51: Patterns aligned vertically and sprued to a horizontal bar

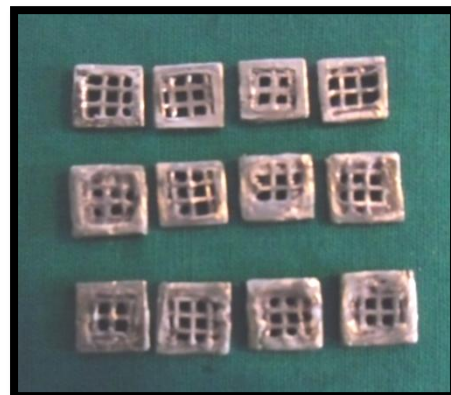


Fig.52: Finished Ti-6Al-4V samples

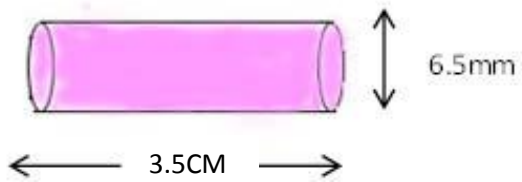


Fig.53a: Line diagram showing cylindrical acrylic extension dimensions

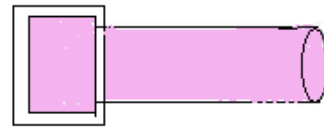


Fig.53b: Line diagram showing waxed up alloy sample



Fig.53c: Waxed-up alloy samples



Fig.54: Invested waxed-up alloy samples



Fig.55: After dewaxing, invested alloy samples in flask base cylindrical mold spaces in the flask body



Fig.56a: Air abraded samples, 56b: Alloy Primer application



Fig.57: Deflasked samples



Fig.58: Finished samples



Fig.59a: Samples in the separate, labeled containers, 59b: Samples in the incubator



Fig.60: Samples in the Thermocycler



Fig.61: Sample fixed to the sample fixture of Universal Testing machine



Fig.62: Tested Samples



Fig.63: Samples in the gold sputtering machine prior to SEM



RESULTS

The present in-vitro study was conducted, to comparatively evaluate the shear bond strength of heat polymerized acrylic resin to Co-Cr and Ti-6Al-4V alloys with two different surface treatments after being subjected to aging and thermocycling and correlated with quantitative 3-D surface texture analysis of treated alloy samples along with pre and post SEM analyses.

44 samples with dimensions of 1cm x 1cm x 1.6 mm were obtained of which 22 samples were obtained with Co-Cr alloy and 22 samples were obtained with Ti-6Al-4V alloy. The samples were divided into four groups comprising of 11 samples each. The groups were designated as Group Ia, Ib, IIa and IIb.

Group Ia samples were subjected to air abrasion with 50 μ m alumina prior to acrylisation.

Group Ib samples were subjected to air abrasion with 50 μ m alumina followed by Alloy Primer application prior to acrylisation.

Group IIa samples were subjected to air abrasion with 50 μ m alumina prior to acrylisation.

Group IIb samples were subjected to air abrasion with 50 μ m alumina followed by Alloy Primer application prior to acrylisation.

10 samples of each group were acrylised after their respective surface treatments with heat cure Polymethylmethacrylate denture base resin. All acrylized samples were subjected to aging for 3 days and thermocycling. After thermocycling,

the samples were subjected to shear bond strength test in Universal Testing Machine. The results obtained were tabulated & subjected to statistical analysis.

One representative surface treated alloy sample from each test group was quantitatively and qualitatively evaluated for surface roughness and surface topography, using 3-D surface profilometer and scanning electron microscope respectively. One representative tested sample from each test group was qualitatively analyzed using SEM for assessing the failure mode.

The following results were drawn from the study:

Tables 1 to 4 show the Basic values and Mean values of shear bond strength in Mpa for acrylised samples of Group Ia, IIa, IIa and IIb.

Table 5 shows the comparison of mean shear bond strengths and standard deviation between Group Ia and Group Ib.

Table 6 shows the comparison of mean shear bond strengths and standard deviation between Group IIa and Group IIb.

Table 7 shows the comparison of mean shear bond strengths and standard deviation between Group Ia and Group IIa.

Table 8 shows the comparison of mean shear bond strengths and standard deviation between Group Ib and Group IIb.

TABLE 1: Basic values and mean value of shear bond strength in Mpa for acrylised samples of Group Ia

S.No	Shear Bond Strength in Mpa
1	2.29
2	3.09
3	2.99
4	2.89
5	2.68
6	1.89
7	2.26
8	2.58
9	2.4
10	2.9
Mean	2.5970

TABLE 2: Basic values and mean value of shear bond strength in Mpa for acrylised samples of Group Ib

S.No	Shear Bond Strength in Mpa
1	7
2	6.5
3	6.69
4	6.29
5	6.79
6	6.13
7	6.88
8	7.07
9	6.4
10	8
Mean	6.7750

TABLE 3: Basic values and mean value of shear bond strength in Mpa for acrylised samples of Group IIa

S.No	Shear Bond Strength in Mpa
1	1.7
2	1.9
3	1.5
4	1.54
5	1.3
6	1.75
7	1.65
8	1.74
9	1.73
10	1.34
Mean	1.6150

TABLE 4: Basic values and mean value of shear bond strength in Mpa for acrylised samples of Group IIb

S.No	Shear Bond Strength in Mpa
1	4.99
2	5.29
3	5.71
4	5.63
5	5.61
6	4.91
7	4.5
8	5.37
9	5.7
10	5.4
Mean	5.3110

Table 5: Comparison of mean shear bond strengths of Group Ia with Group Ib

Variable	N	Mean	S.D	p-value
Group Ia	10	2.5970	0.3842	0.05*
Group Ib	10	6.7750	0.5296	

Note: * denotes significance at 5% level (highly significant)

INFERENCE: The mean shear bond strength of Group Ia was 2.5970 Mpa and Group Ib was 6.7750 Mpa. On comparison between the two groups, the results were found to be statistically significant.

Table 6: Comparison of mean shear bond strengths of Group IIa with Group IIb

Variable	N	Mean	S.D	p-value
Group IIa	10	1.6150	0.1916	0.05*
Group IIb	10	5.3110	0.3993	

Note: * denotes significance at 5% level (highly significant)

INFERENCE: The mean shear bond strength of Group IIa was 1.6150 Mpa and Group IIb was 5.3110 Mpa. On comparison between the two groups, the results were found to be statistically significant.

Table 7: Comparison of mean shear bond strengths of Group Ia with Group IIa

Variable	N	Mean	S.D	p-value
Group Ia	10	2.5970	0.3842	0.05*
Group IIa	10	1.6150	0.1916	

Note: * denotes significance at 5% level (highly significant)

INFERENCE: The mean shear bond strength of Group Ia was 2.5970 Mpa and Group IIa was 1.6150 Mpa. On comparison between the two groups, the results were found to be statistically significant

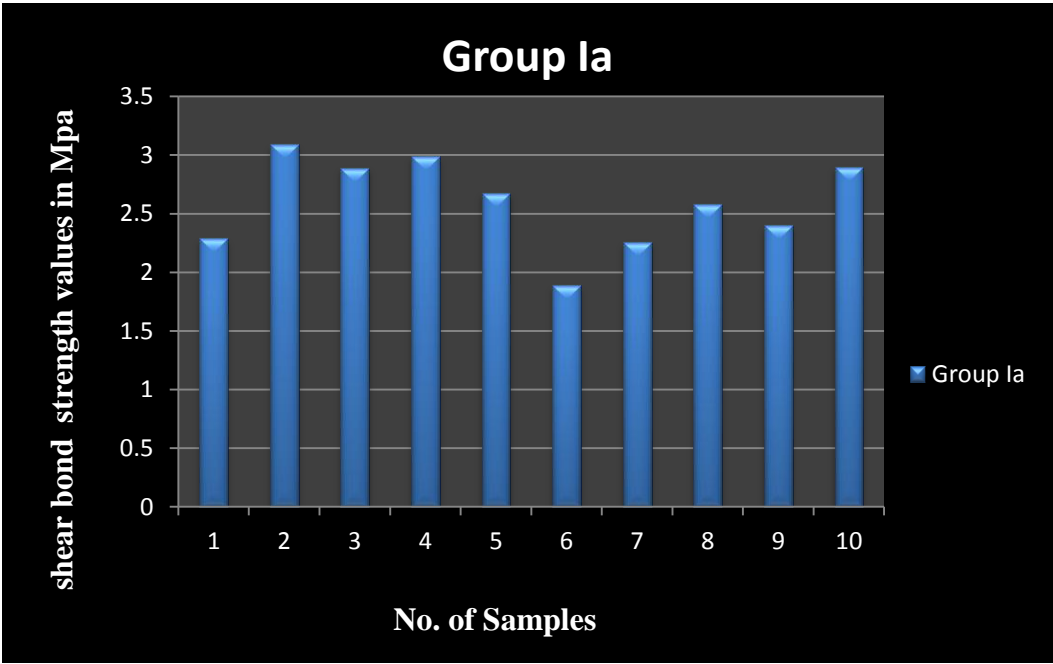
Table 8: Comparison of mean shear bond strengths of Group Ib with Group IIb

Variable	N	Mean	S.D	p-value
Group Ib	10	6.7750	0.5296	0.05*
Group IIb	10	5.3110	0.3993	

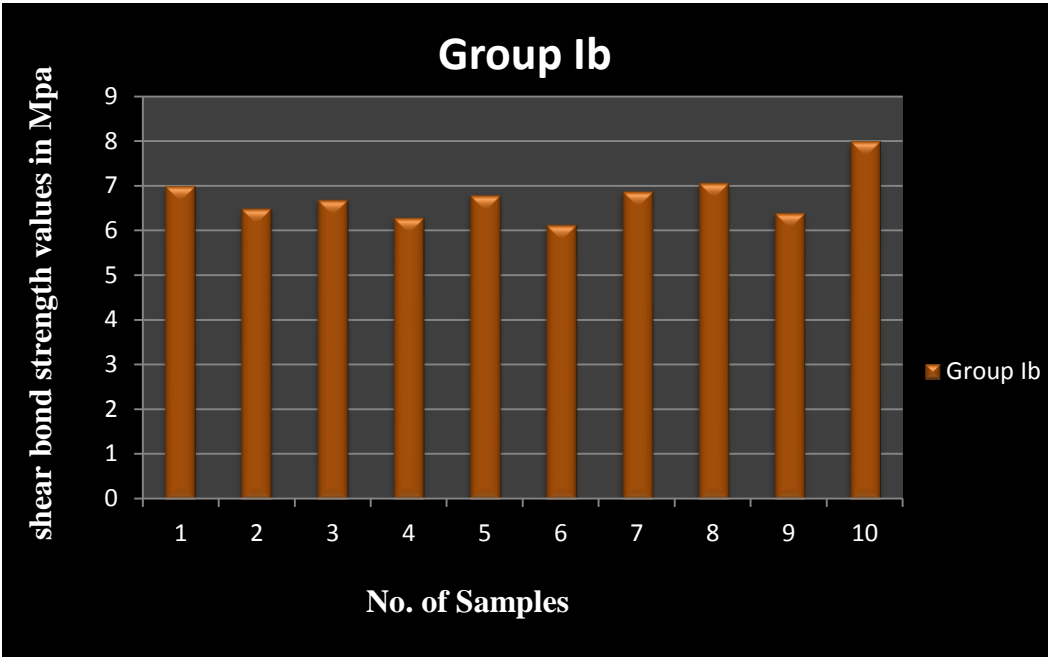
Note: * denotes significance at 5% level (highly significant)

INFERENCE: The mean shear bond strength of Group Ib was 6.7750 Mpa and Group IIb was 5.3110 Mpa. On comparison between the two groups, the results were found to be statistically significant.

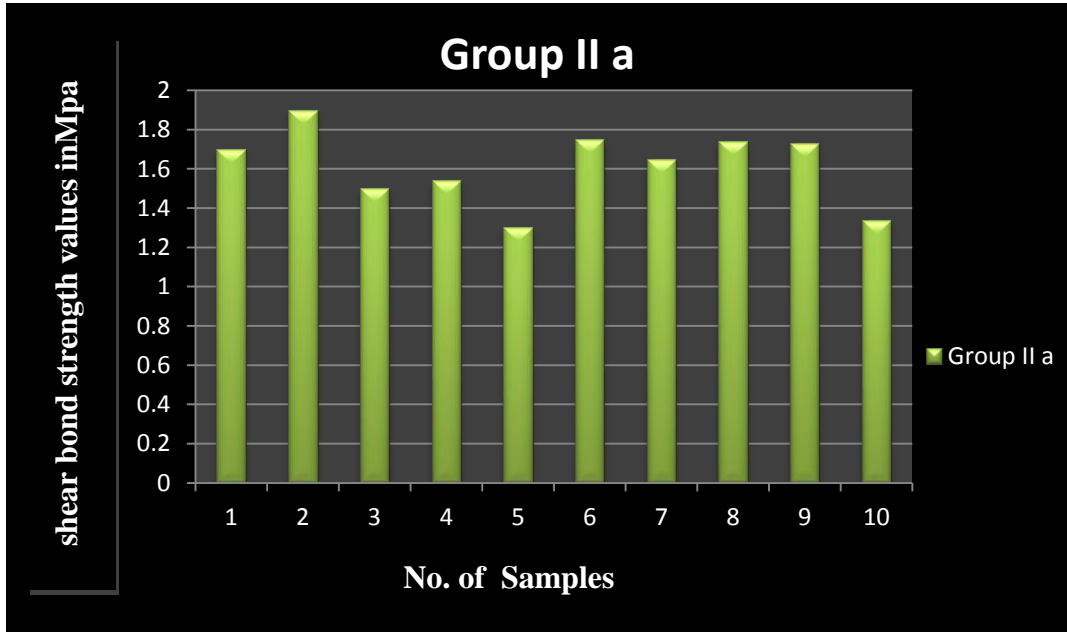
Graph 1: Basic values of shear bond strength in Mpa for Group Ia



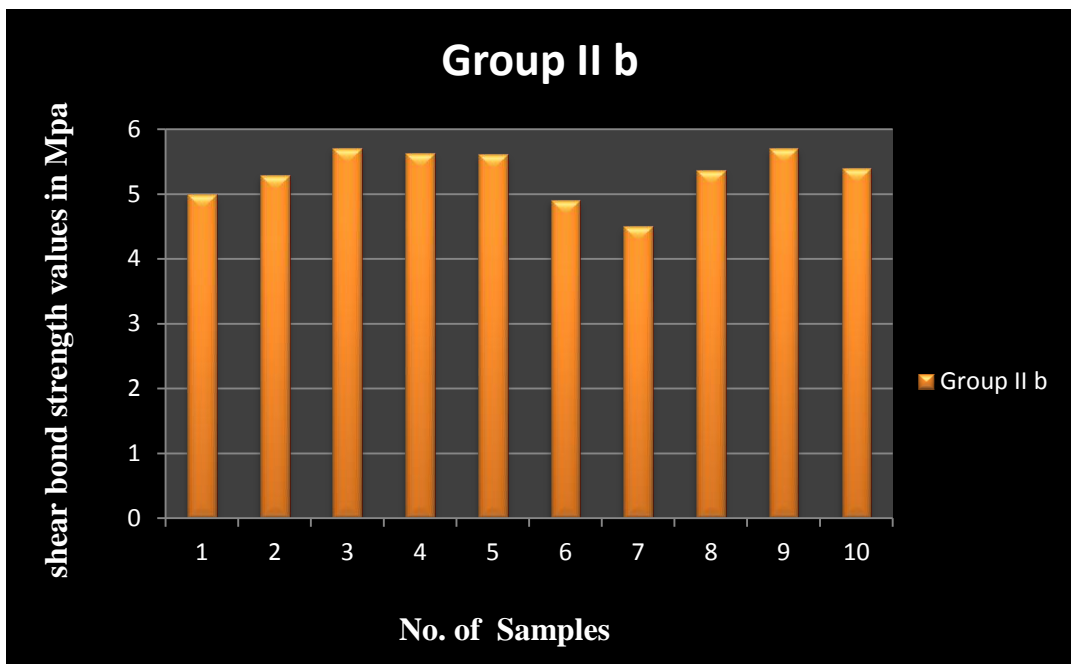
Graph 2: Basic values of shear bond strength in Mpa for Group Ib



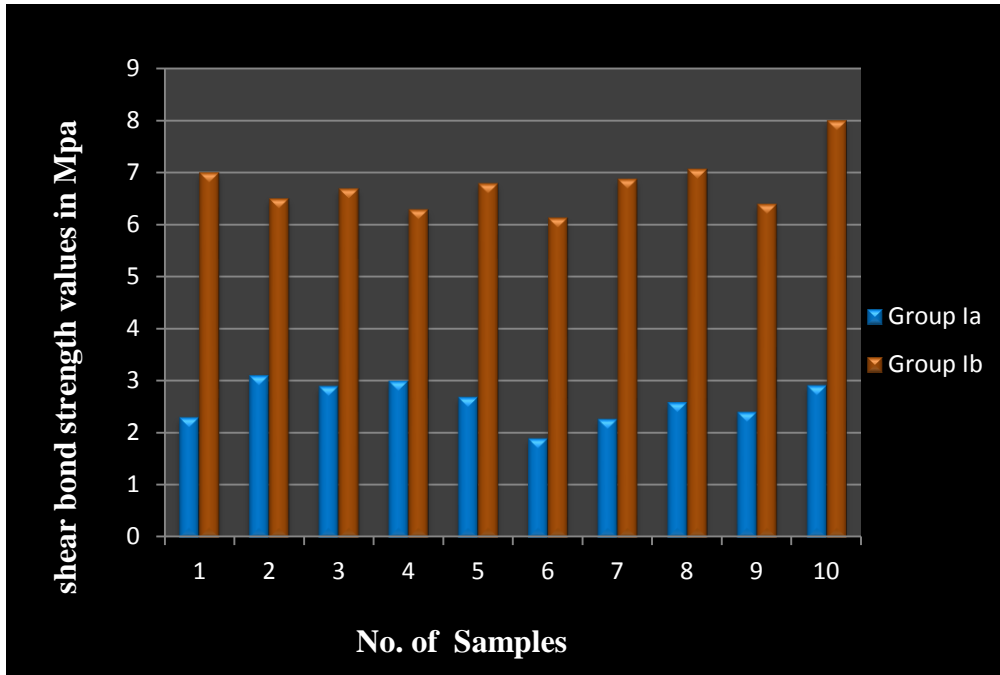
Graph 3: Basic values of shear bond strength in Mpa for Group IIa



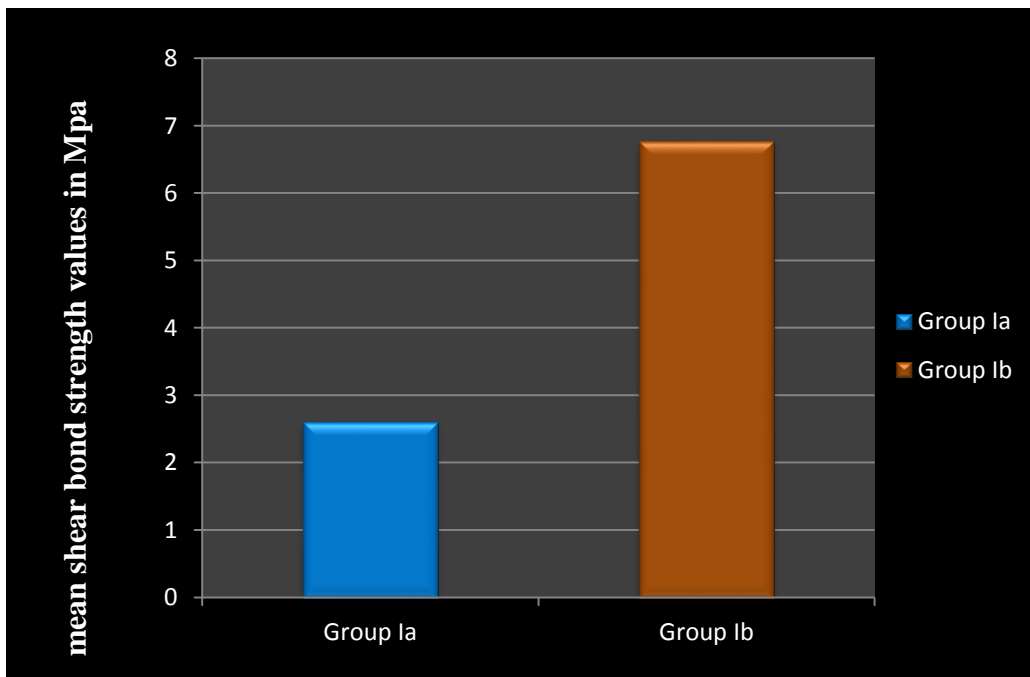
Graph 4: Basic values of shear bond strength in Mpa for Group IIb



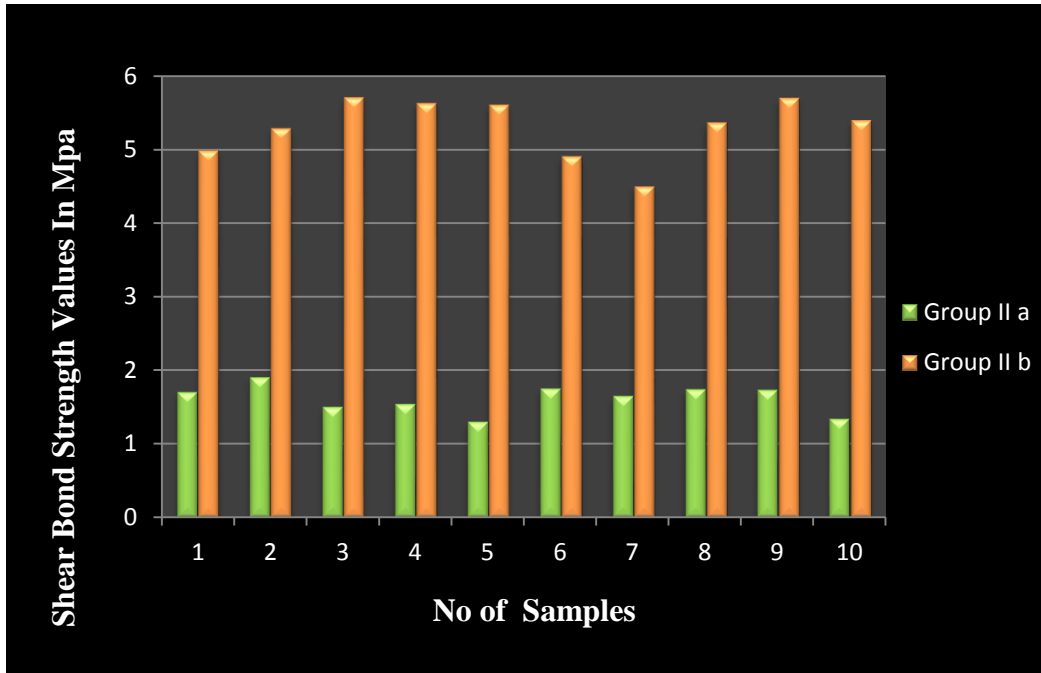
Graph 6: Comparison of shear bond strength values of Group Ia with Group Ib



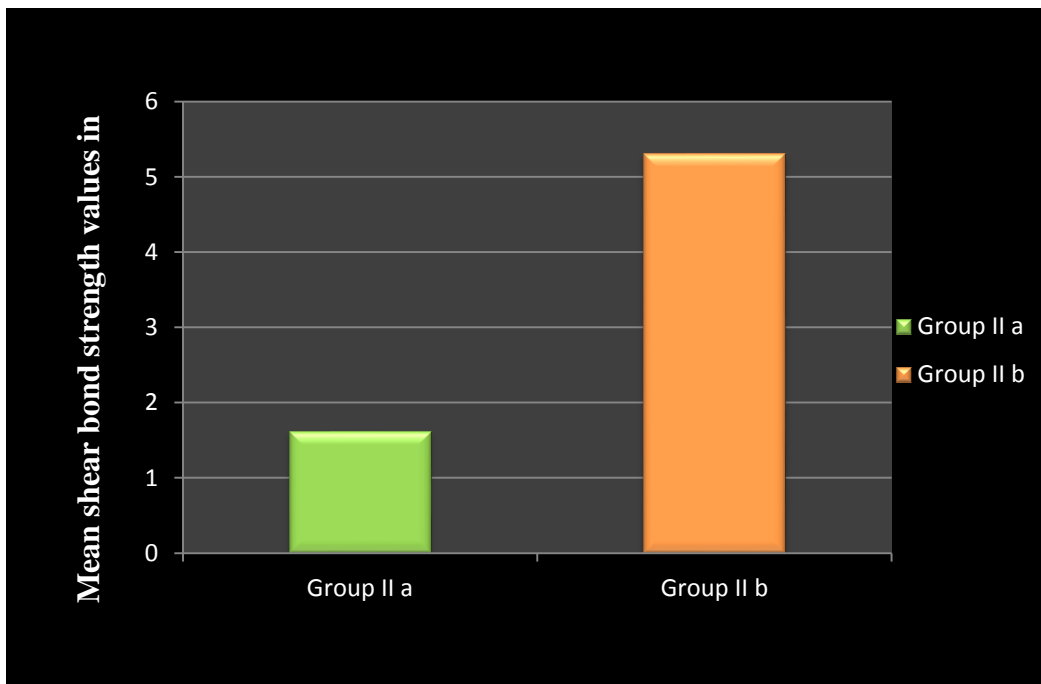
Graph 7: Comparison of mean shear bond strength values of Group Ia with Group Ib



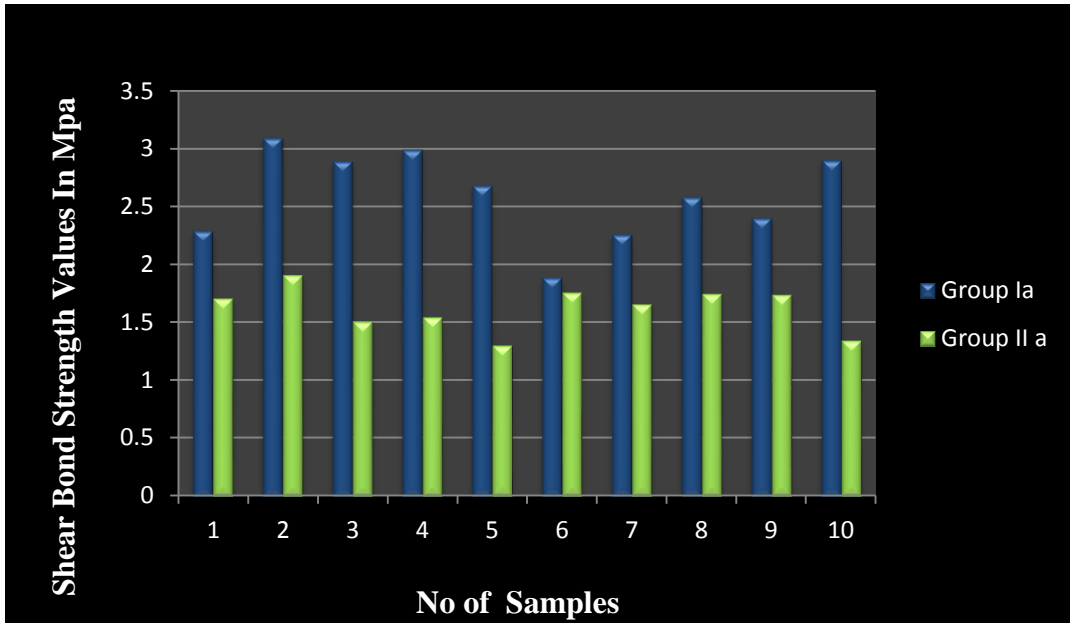
Graph 8: Comparison of shear bond strength values of Group IIa with Group IIb



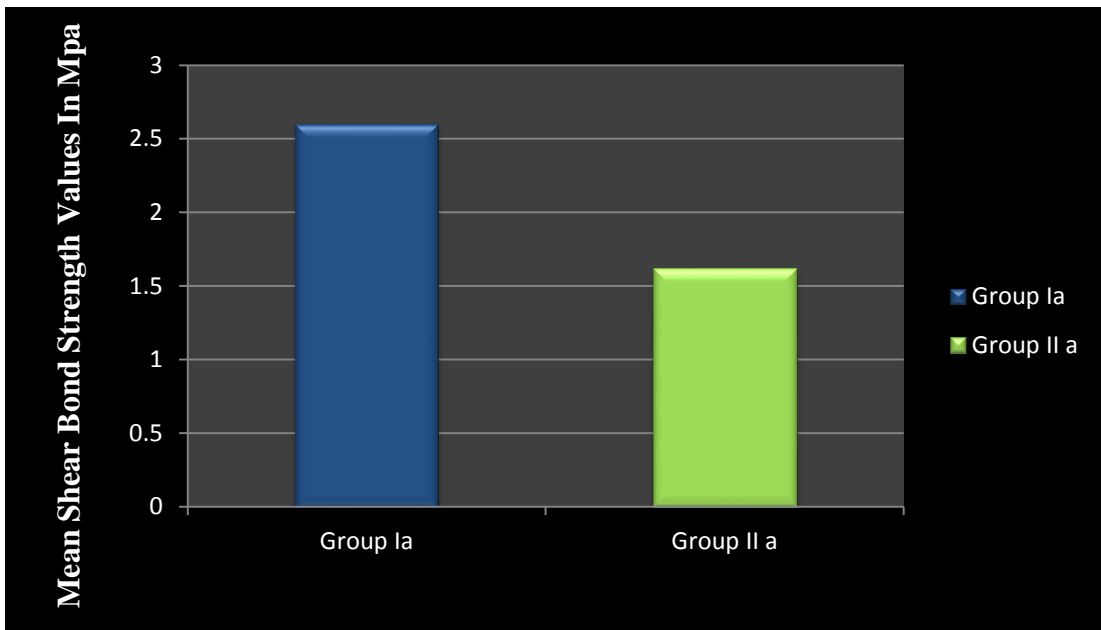
Graph 9: Comparison of mean shear bond strength values of Group IIa with Group IIb



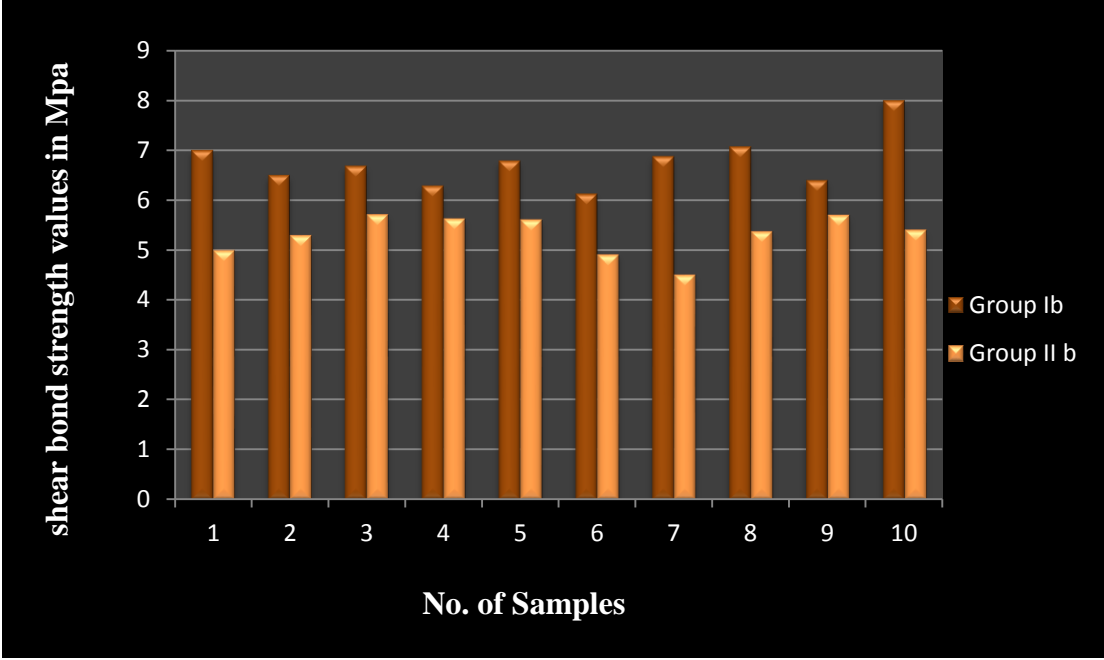
Graph 10: Comparison of shear bond strength values of Group Ia with Group IIa



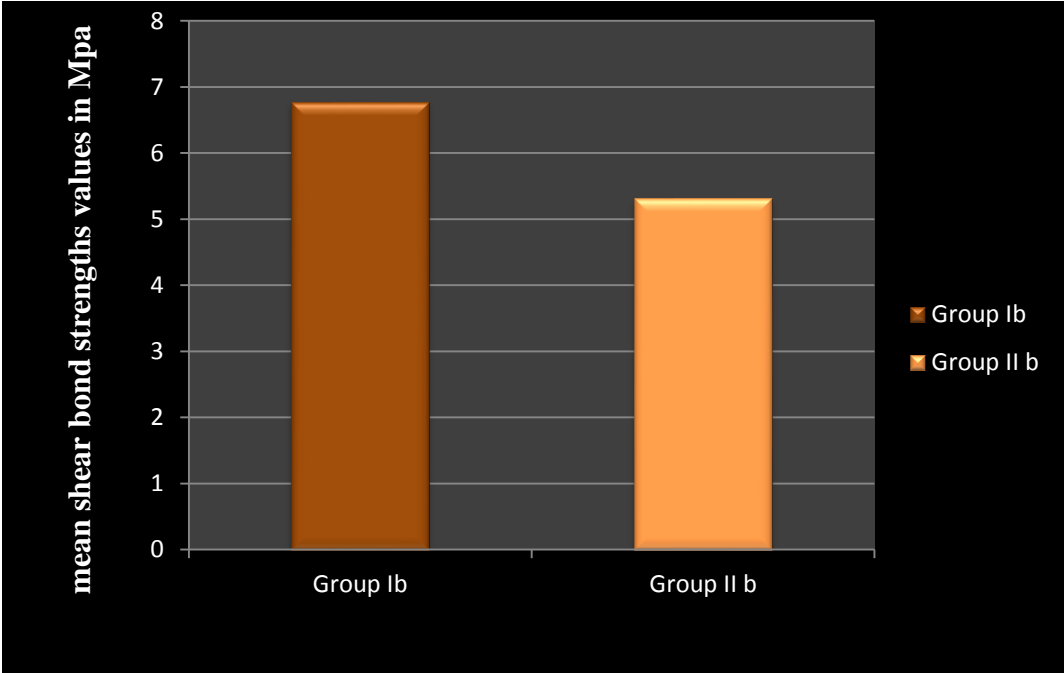
Graph 11: Comparison of mean shear bond strength values of Group Ia with Group IIa



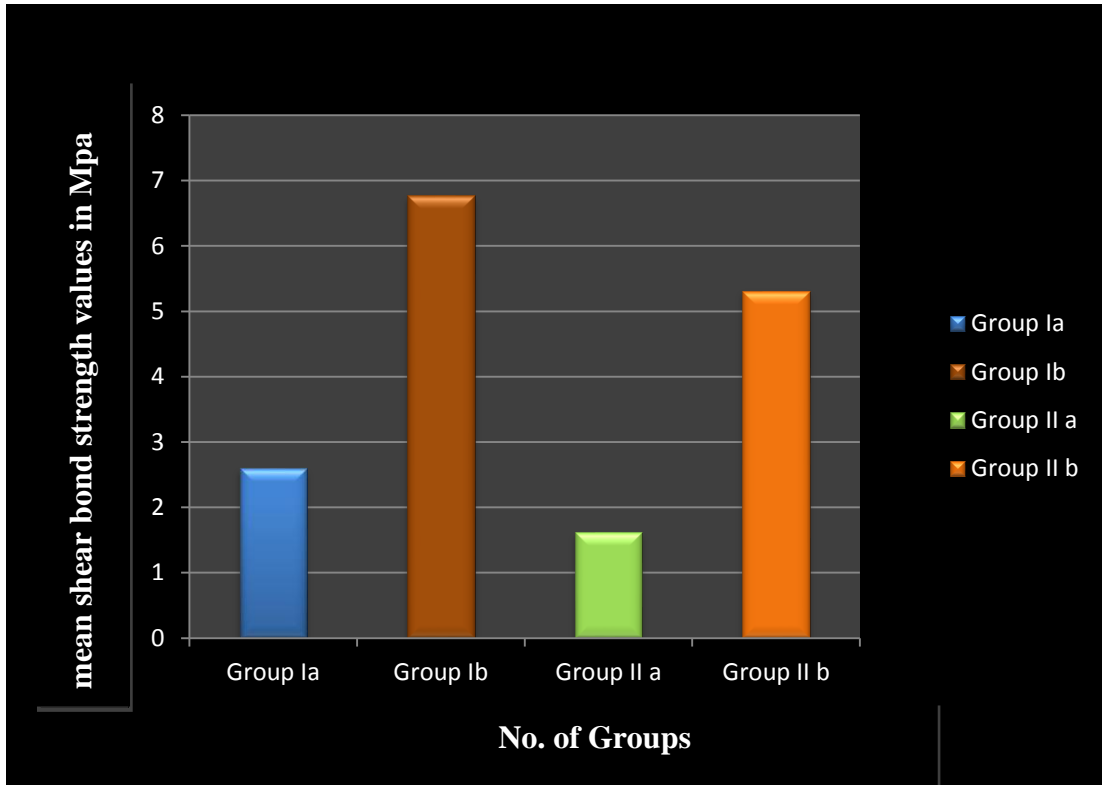
Graph 12: Comparison of shear bond strength values of Group Ib with Group IIb



Graph 13: Comparison of mean shear bond strength values of Group Ib with Group IIb



Graph 5: Comparison of mean shear bond strength values of groups Ia, Ib, IIa and IIb



**Quantitative 3-D surface texture analysis of surface treated alloy sample
of Group Ia by 3-D Surface Profilometry**

Group Ia

3-D view

Advanced 3-D view

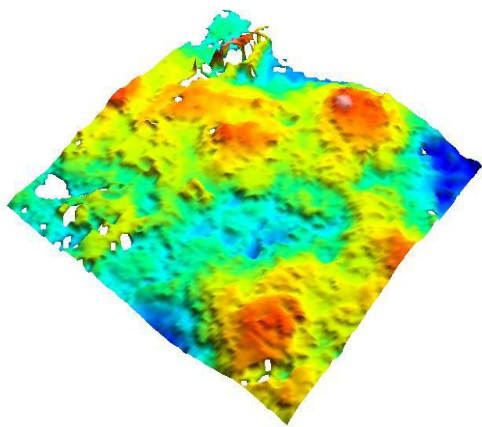


Fig.64

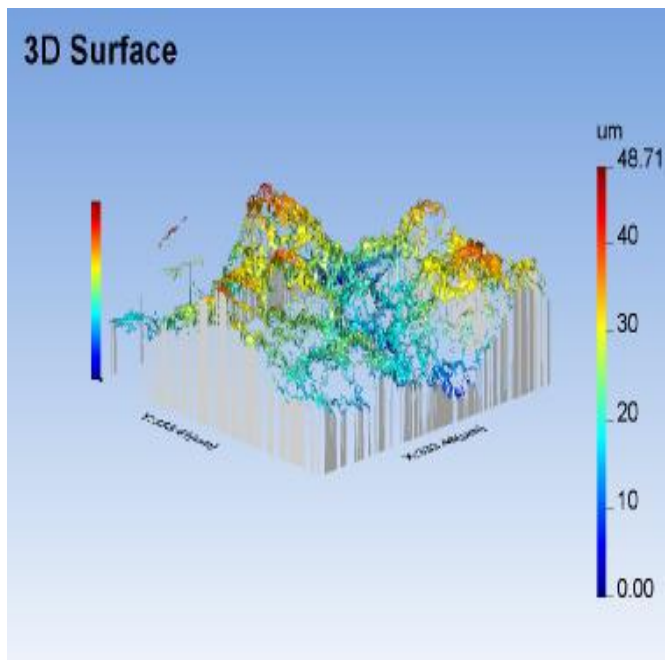


Fig.65

Parameters	Values in μm
Rp	1.57
Rv	1.99
Ra	0.514

Inference (Group Ia) : 3-D and advanced 3-D view images (Figs 64 & 65) of surface treated alloy surface with air abrasion shows the irregular distribution and poorly defined peaks and valleys on the alloy surface and an average surface roughness value (Ra value) of 0.514 μm .

**Quantitative 3-D surface texture analysis of surface treated alloy sample
of Group Ib by 3-D Surface Profilometry**

Group Ib

3-D view

Advanced 3-D view

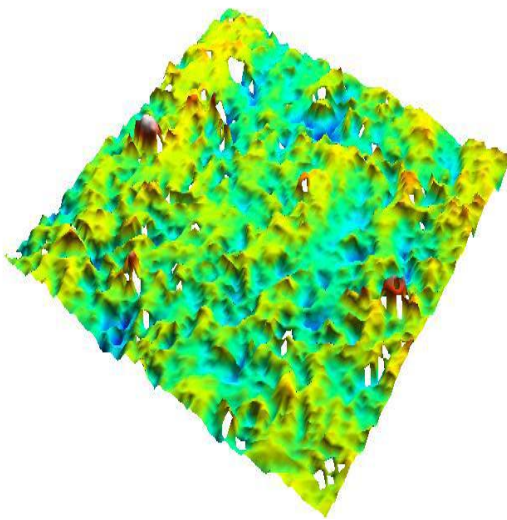


Fig.66

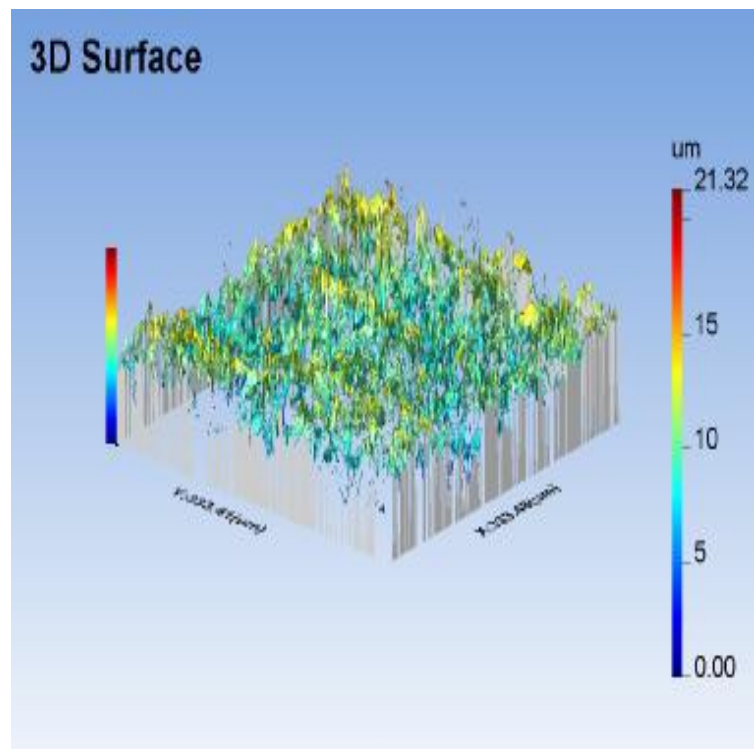


Fig. 67

Parameters	Values in μm
Rp	1.60
Rv	2.29
Ra	0.672

Inference (Group Ib): 3-D and advanced 3-D view images (Figs 66 & 67) of surface treated alloy sample with air abrasion followed by alloy primer application shows the uniformly distributed and well defined peaks and valleys on the alloy surface and an average surface roughness value (Ra value) of 0.672 μm .

**Quantitative 3-D surface texture analysis of surface treated alloy sample
of Group IIa by 3-D Surface Profilometry**

Group IIa

3-D view

Advanced 3-D view

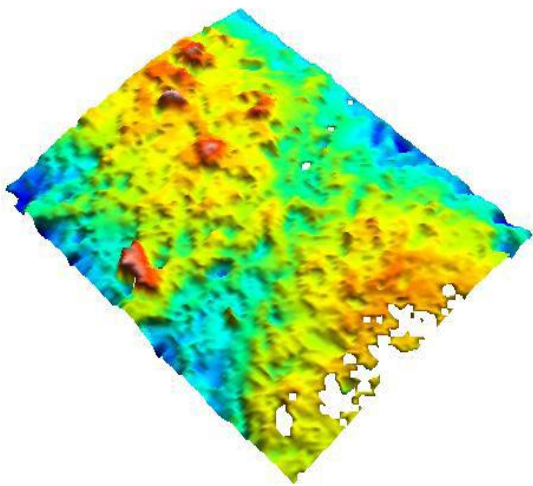


Fig.68

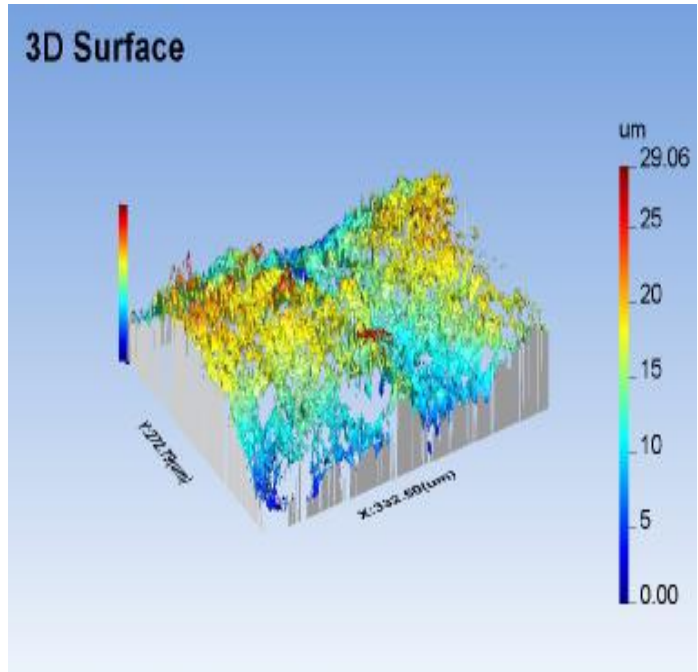


Fig.69

Parameters	Values in μm
Rp	1.77
Rv	2.30
Ra	0.534

Inference (Group IIa) : 3-D and advanced 3-D view images (Figs 68 & 69) of surface treated alloy surface with air abrasion shows the patchy distribution of poorly defined peaks and valleys on the alloy surface and an average surface roughness value (Ra value) of 0.534 μm .

**Quantitative 3-D surface texture analysis of surface treated alloy sample
of Group IIb by 3-D Surface Profilometry**

Group IIb

3-D view

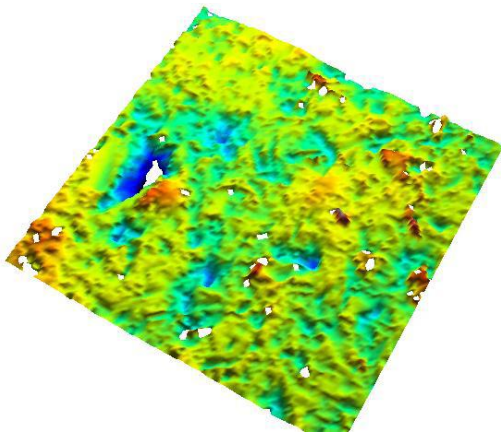


Fig.70

Advanced 3-D view

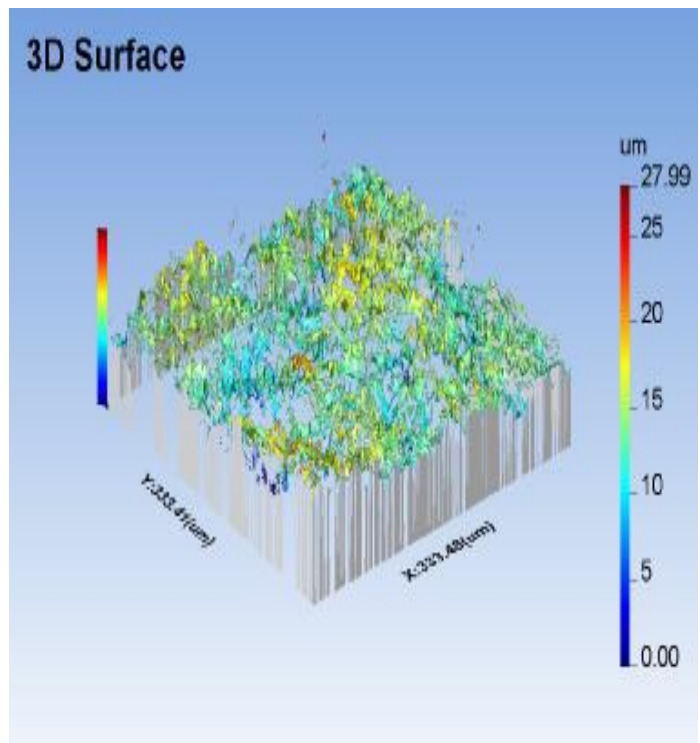


Fig.71

Parameters	Values in μm
Rp	2.12
Rv	2.73
Ra	0.700

Inference (Group IIb): 3-D and advanced 3-D view images (Figs 70 & 71) of surface treated alloy samples with air abrasion followed by alloy primer application shows peaks and valleys that are evenly distributed on the alloy surface and an average surface roughness value (Ra value) of 0.700 μm .

Qualitative analysis of surface topography of surface treated Co-Cr alloy samples (Groups Ia and Ib) by scanning electron microscope under 10x and 500x magnifications:

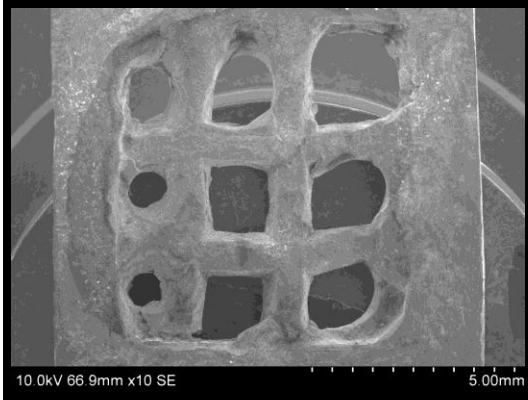


Fig.72: Group Ia pretest SEM under 10x

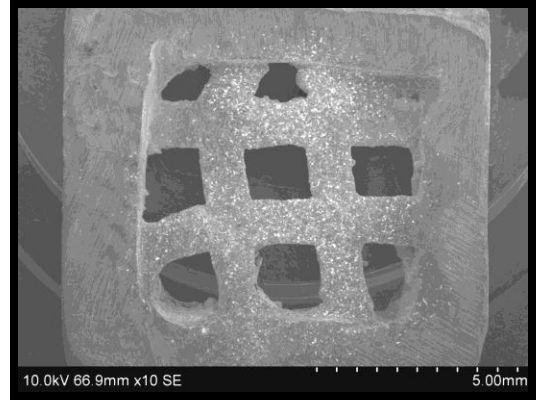


Fig.73: Group Ib pretest SEM under 10x

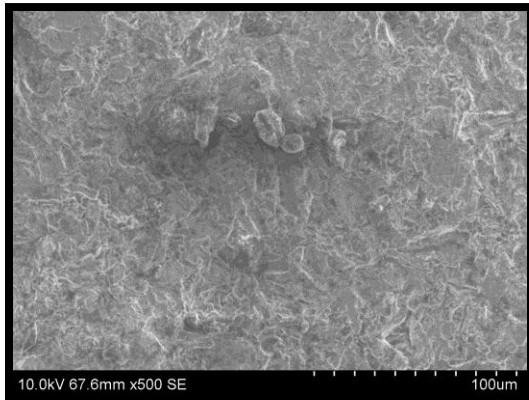


Fig.74: Group Ia pretest SEM under 500x

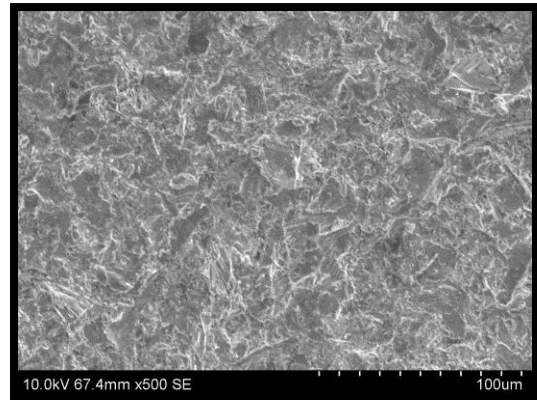


Fig.75: Group Ib pretest SEM under 500x

SEM inferences of Groups Ia and Ib test samples after respective surface treatments:

Under 10x magnification, Group Ib test sample shows uniform frosty appearance as compared to Group Ia (Figs.72 & 73). Under 500x magnification, Group Ia test sample shows moderately micro-roughened surface topography with poorly defined peaks and valleys (Fig.74). In contrast, Group Ib test sample shows a micro-roughened surface topography with more number of peaks and valleys that are distributed uniformly throughout the surface (Fig.75).

Qualitative analysis of surface topography of surface treated Ti-6Al-4V alloy samples (Groups IIa and IIb) by scanning electron microscope under 10x and 500x magnifications:

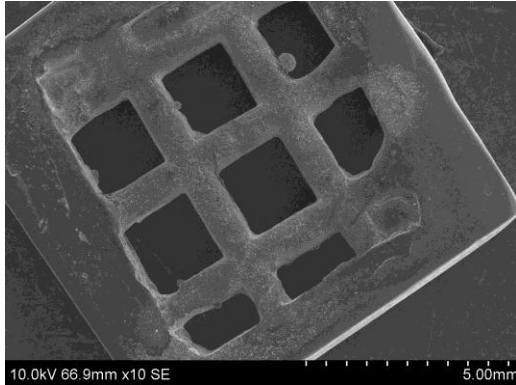


Fig.76: Group IIa pretest SEM under 10x

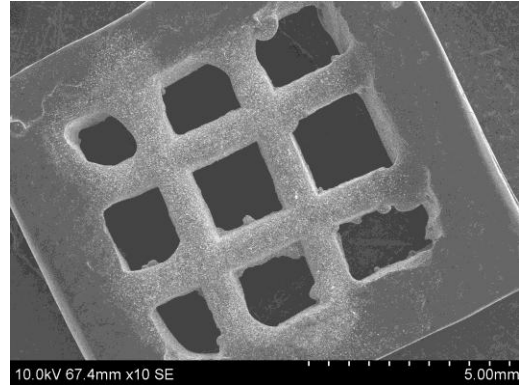


Fig.77: Group IIb pretest SEM under 10x

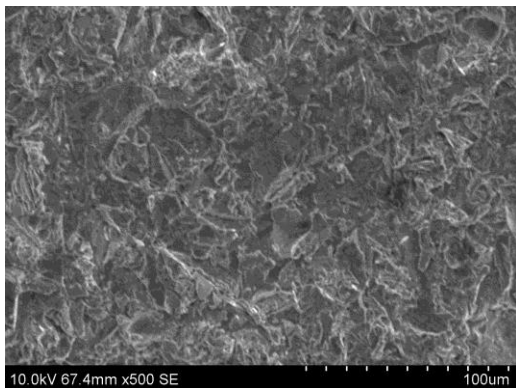


Fig.78: Group IIa pretest SEM under 500x

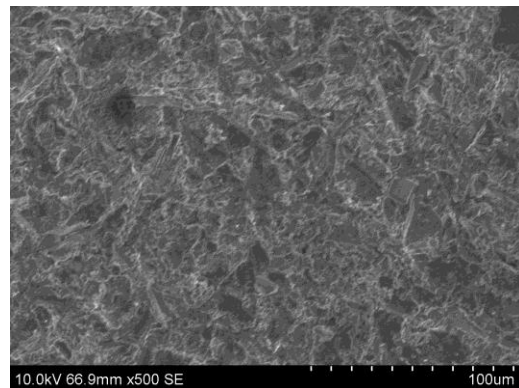


Fig.79: Group IIb pretest SEM under 500x

SEM inferences of Groups IIa and IIb test samples after respective surface treatments:

Under 10x magnification, Group IIb test sample shows a well distributed, visible, uniform frosty appearance of the surface as compared to Group IIa test sample (Figs 76 & 77). Under 500x magnification, Group IIa test sample subjected to air abrasion, shows irregularly abraded surface topography (Fig.78). In contrast, Group IIb test sample shows a uniformly micro roughened surface topography with well defined peaks and valleys (Fig.79).

Qualitative analysis of the mode of failure of the tested Co-Cr alloy samples (Group Ia) by scanning electron microscopy under 10x, 250x, 500x and 1000x magnifications:

Group Ia : SEM of fractured alloy surface

SEM of fractured acrylic surface

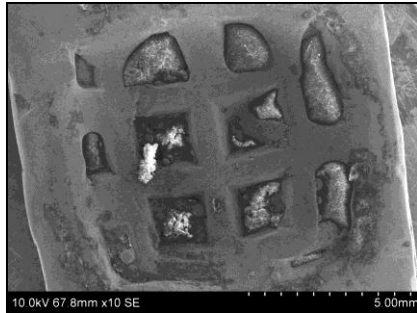


Fig.80: Under 10x

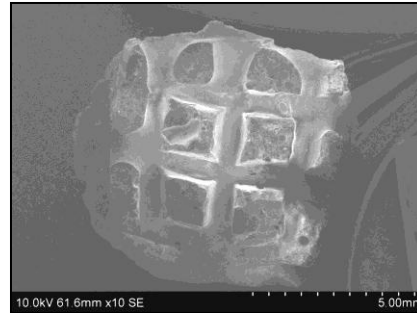


Fig.84: Under 10x

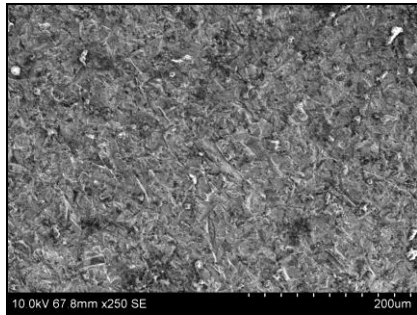


Fig.81: Under 250x

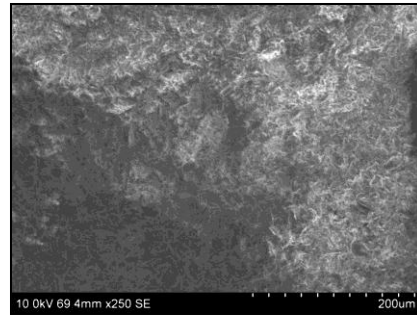


Fig.85: Under 250x

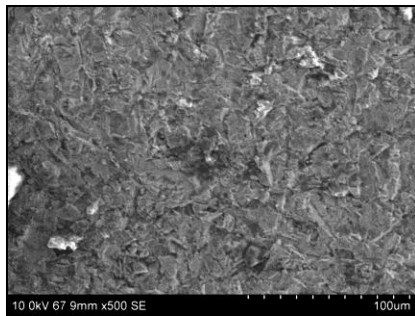


Fig.82: Under 500x

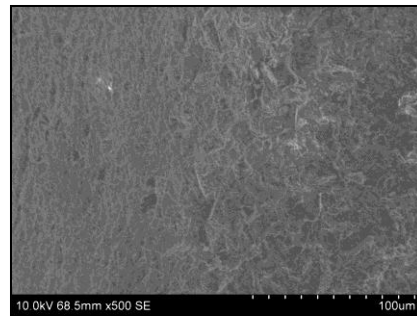


Fig.86: Under 500x

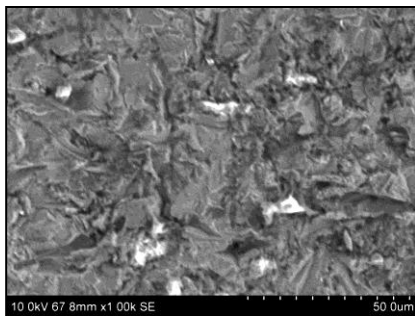


Fig.83: Under 1000x

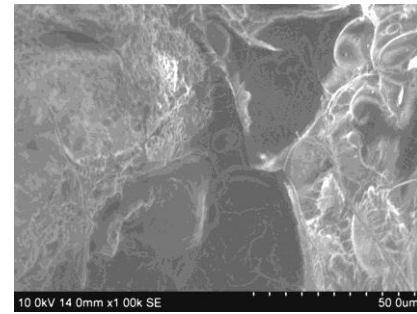


Fig.87: Under 1000x

Qualitative analysis of the mode of failure of the tested Co-Cr alloy samples (Group Ib) by scanning electron microscopy under 10x, 250x, 500x and 1000x magnifications:

Group Ib : SEM of fractured alloy surface

SEM of fractured acrylic surface

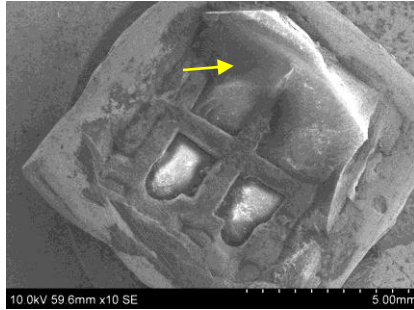


Fig.88: Under 10x

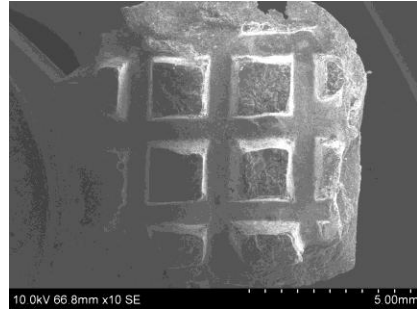


Fig.92: Under 10x

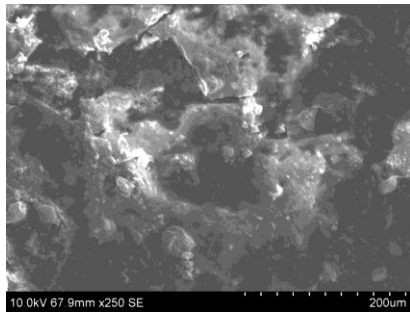


Fig.89: Under 250x

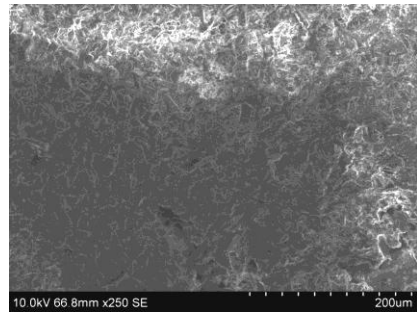


Fig.93: Under 250x

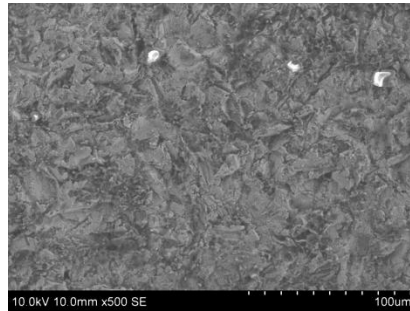


Fig.90: Under 500x

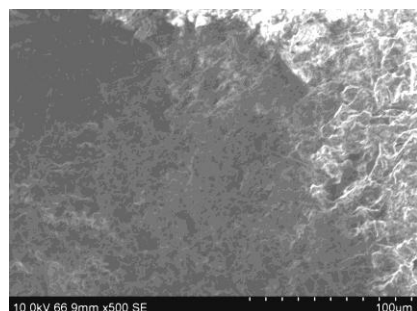


Fig.94: Under 500x

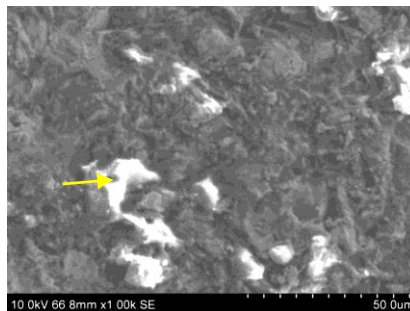


Fig.91: Under 1000x

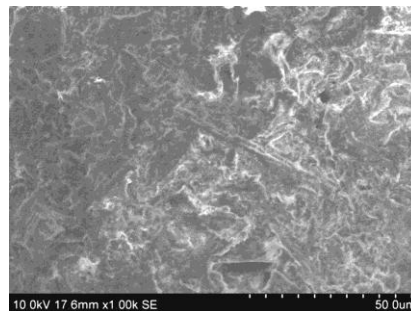


Fig.95: Under 1000x

SEM inferences of Groups Ia and Ib test samples after shear bond strength testing:

The SEM photomicrograph of the fractured alloy portion of the Group Ia sample exhibited predominantly an adhesive failure pattern. Under 10x magnification, acrylic resin on the under surface of the mesh is visible through the mesh design (Fig.80). However very minimal or no visible resin tags are present on the alloy mesh surface. Under 250x, 500x and 1000x magnifications, group Ia sample shows the micro roughened alloy surface. Sparse specks of resin are visible (Figs 81, 82 & 83).

In contrast, the SEM photomicrograph of the fractured alloy portion of the Group Ib sample exhibited a mixed adhesive and cohesive failure pattern. The predominant mode of failure was cohesive within the acrylic resin, with residual tags of acrylic resin attached on the alloy surface. Under 10x magnification, Group Ib sample shows acrylic resin tags projecting from the mesh surface (Fig.88). Under 250x, 500x and 1000x magnifications, Group Ib sample shows a heterogenous surface topography with distributed presence of acrylic resin attached to the alloy surface (Figs 89, 90 & 91).

SEM photomicrograph of the fractured acrylic portion of the Group Ia sample revealed a mixed surface topography with predominantly smoother and some roughened areas under 250x, 500x and 1000x magnifications (Figs 85, 86 & 87). Under 10x magnification there is a well-defined acrylic mesh structure with no alloy tags indicating an adhesive failure pattern (Fig 84).

In comparison, the SEM photomicrograph of the fractured acrylic portion of the Group Ib sample under 10x magnification shows clearly visible fractured acrylic corresponding to the mesh surface (Fig.92). Under 250x, 500x and 1000x magnifications, the acrylic surface topography is rough indicating cohesive fracture within the acrylic resin (Figs 93, 94 & 95)

Qualitative analysis of the mode of failure of the tested Ti-6Al-4V samples (Group IIa) by scanning electron microscopy under 10x,250x and 500x and 1000x magnifications:

Group IIa : SEM of fractured alloy surface

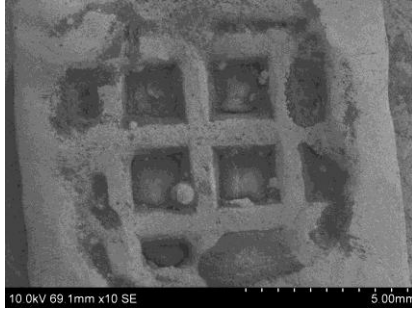


Fig.96: Under 10x

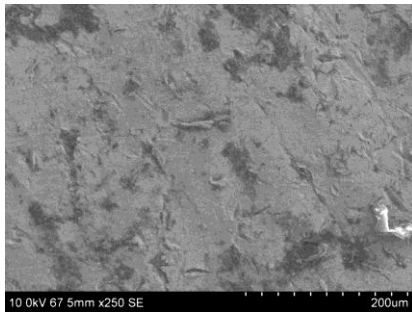


Fig.97: Under 250x

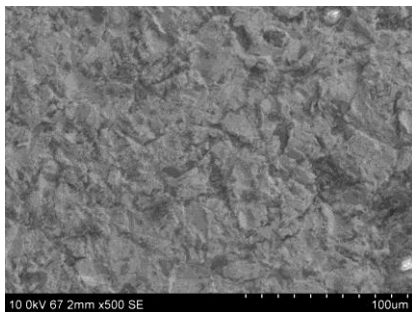


Fig.98: Under 500x

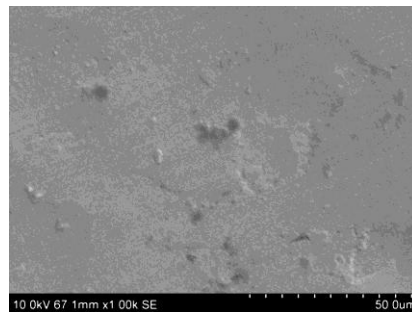


Fig.99: Under 1000x

SEM of fractured acrylic sample

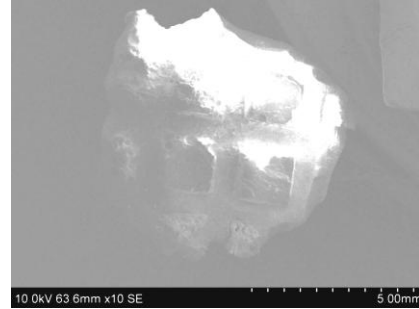


Fig.100: Under 10x

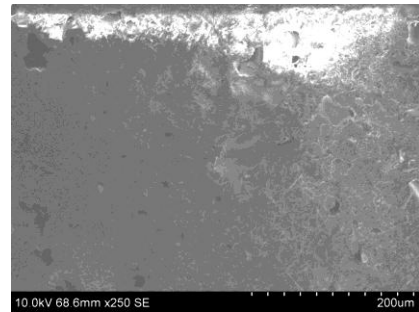


Fig.101: Under 250x

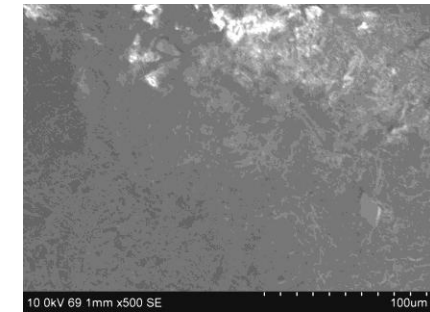


Fig.102: Under 500x

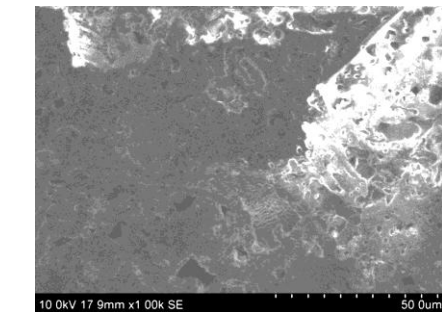


Fig.103: Under 1000x

Qualitative analysis of the mode of failure of the tested Ti-6Al-4V samples (Group IIb) by scanning electron microscopy under 10x, 250x, 500x and 1000x magnifications:

Group IIb: SEM of fractured alloy surface

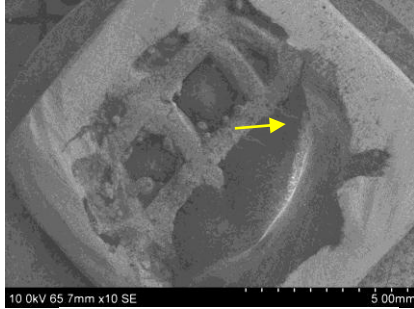


Fig.104: Under 10x

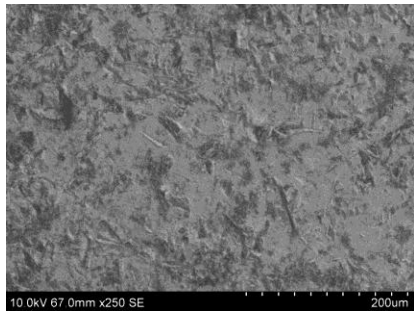


Fig.105: Under 250x



Fig.106: Under 500x

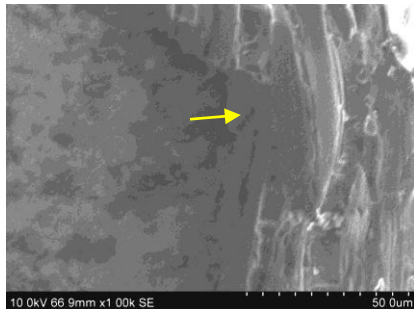


Fig.107: Under 1000x

SEM of fractured acrylic sample



Fig.108: Under 10x

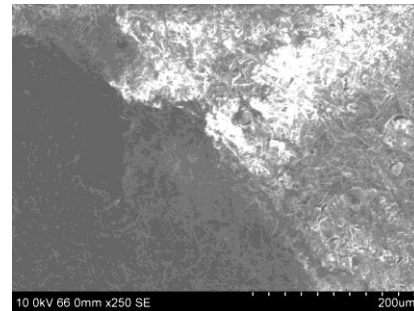


Fig.109: Under 250x

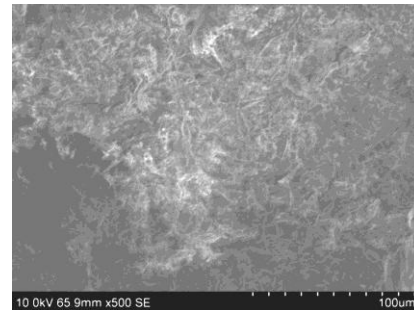


Fig.110: Under 500x

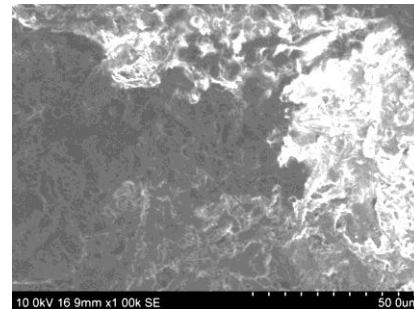


Fig.111: Under 1000x

SEM inferences of Groups IIa and IIb test samples after shear bond strength testing:

The SEM photomicrograph of the fractured alloy portion of the Group IIa sample exhibited predominantly an adhesive failure pattern. Under 10x magnification, acrylic resin on the under surface of the mesh is visible through the mesh design (Fig.96). However very minimal or no visible resin tags are present on the alloy mesh surface. Under 250x, 500x and 1000x magnifications, group IIa sample shows the micro roughened alloy surface (Figs. 97, 98 & 99).

In contrast, the SEM photomicrograph of the fractured alloy portion of the Group IIb sample exhibited a mixed adhesive and cohesive failure pattern. The predominant mode of failure was cohesive within the acrylic resin, with residual tags of acrylic resin attached on the alloy surface. Under 10x magnification, Group IIb sample shows acrylic resin tags projecting from the mesh surface (Fig.104). Under 250x, 500x and 1000x magnifications, Group IIb sample shows a heterogenous surface topography with well defined, visible tags of acrylic resin attached to the alloy surface (Figs.105,106 & 107).

SEM photomicrograph of the fractured acrylic portion of the Group IIa sample revealed a predominantly smoother surface topography with very few roughened areas under 250x, 500x and 1000x magnifications (Figs 101,102 & 103). Under 10x magnification there is a well defined acrylic mesh structure with no alloy tags indicating an adhesive failure pattern (Fig.100).

In comparison, the SEM photomicrograph of the fractured acrylic portion of the Group IIb sample under 10x magnification shows clearly visible fractured acrylic corresponding to the mesh surface (Fig.108). Under 250x, 500x and 1000x magnifications, the acrylic surface topography is predominantly rough indicating cohesive fracture within the acrylic resin (Figs. 109,110 &111).

DISCUSSION

Removable partial dentures (RPDs) are commonly constructed with acrylic resin and metal alloys.^{18,32,48} Although the methods employed in the construction of removable partial dentures have not altered critically in the last decades, the types of alloys preferred for the construction of framework have undergone a transition.^{7,48}

Earlier, type IV gold alloys were used for RPD framework because they are non-toxic, non-allergic and corrosion resistant. However, disadvantages such as their low modulus of elasticity and higher costs led to the introduction of base metal alloys for the same purpose^{2,6}. Co-Cr alloys are widely used because of their physical strength, mechanical properties, corrosion resistance and lower costs. Difficulties in finishing procedures and presence of elements which may produce sensitivity or allergic reactions in some patients are some of the drawbacks.^{2,21,48}

Recently, titanium and its alloys have been introduced for the construction of RPD frameworks with an aim to reduce the reported problems with Co-Cr alloys. Their excellent corrosion resistance, biocompatibility, strength and ductility render them as ideal biomaterials for removable partial dentures. Studies have shown that titanium and its alloys are more flexible and have lower fatigue resistance than Co-Cr alloys.^{21,24,28,38,39,41,45}

Heat polymerized polymethylmethacrylate (PMMA) denture base resin is commonly utilized for attaching artificial acrylic teeth to cast partial dentures.^{2,18} Durability of the removable partial denture is dependent upon the bond between acrylic resin and the alloy framework.^{4,18,21,44} Approximately 38% of removable partial denture failures have been linked to fracture at the alloy-acrylic resin interface.⁴ The junction between the alloy and acrylic resin is an area of clinical concern. Denture deflection during use can also cause debonding between the denture base resin and framework, resulting eventually in resin fracture.^{21,37}

The considerable difference in coefficient of thermal expansion between the alloy and acrylic resin leads to microleakage at this junction, resulting in resin discoloration, fluid percolation and deterioration of contact between the alloy and acrylic resin. This creates space between the alloy and resin, where oral debris, microorganisms and stains accumulate.^{32,37,44} The absence of bonding between the unprepared metal surface and acrylic resin interface is well documented.^{44,61} Various metal alloy surface preparations have been suggested to achieve an improved bond.²⁹

Methods for bonding acrylic resin to alloy have been categorized as mechanical, chemical or combination of both. Mechanical methods rely on macromechanical and micromechanical. The macromechanical retention for a denture base resin is usually provided by the framework design in the denture base using beads, nail heads, posts, bars, an open lattice, a mesh or some

macroscopic retention design.^{32,34,37,44,48,61} Boucher and Renner stated that the most common acrylic retention designs were open lattice, preformed mesh and a metal base with bead retention. They endorsed the lattice design.⁹ However studies have shown that it has a high susceptibility to permanent deformation.²⁹ The major disadvantage of macromechanical retention between the denture base resin and alloy framework was poor marginal sealing, permitting seepage of oral fluids between the resin-metal interface leading to the above mentioned sequelae.^{32,34,37,44,48,61}

The micromechanical retention methods include electrolytic etching, gel (acid) etching and air abrasion.⁴⁴ Electrochemical etching improved bond strength and avoided overcontouring of the prosthesis. Zurasky and Duke compared the retentive bond strength of an acid-etched base metal to acrylic resin with that of retentive beads. They found that the bond with the acid etched base was 3.5 times greater than that with bead retention.⁶¹ These techniques are associated with expensive equipment, technique sensitivity and harmful chemicals.^{29,44}

Air abrasion is one of the commonly employed mechanisms of improving the bond strength by providing micromechanical retention. It is an easy-to-accomplish procedure. The metal substrates are roughened by air borne particle abrasion. During the polymerization of denture base resins, polymerization shrinkage occurs, which causes contraction stress of the polymer towards the micro irregularities of the abraded surface.¹⁸ Retention

increases due to the increase in microsurface area thereby increasing the wettability of the resin.⁴⁴

Chemical bonding between the metal framework and the denture base resin is also important. Poor chemical bonding in this area is a significant clinical problem, often introducing adhesive failure and increasing microleakage of oral fluids at the finish line.^{4,6,37,44} Kourtis classified available chemical bonding systems into three main groups according to their mechanism of adhesion to metal: silicate layer coating/silane coupling agents, tin/oxide layer plating and active acrylate monomers as bonding agents.²⁹

The Silicoater system developed by Tiller et al in 1984 was the earliest reported chemical retentive system. An intermediate layer containing silicon dioxide on the metal surface provided sufficient bonding of acrylic resin via a silane bonding agent. NaBadalung et al demonstrated that the bond strength of a silica coated metal was significantly higher than that of sandblasted and electroetched metal.³⁶ However, expensive equipment, time constraints, technique sensitivity were among the disadvantages of the process.^{4,29} Tin plating is relatively easily performed with consistent results, although low bond strengths for base metal alloys have been reported. Sharp B et al reported that tinplating was not effective in reducing the microleakage between the acrylic resin and base metal alloys when used alone or in combination with other surface treatments. Tin plating improved the bond strengths when associated with noble alloys.⁴⁴

Active or functional methacrylate monomers have been synthesized and successfully used as primers for bonding acrylic resin to dental alloys.²⁹ The composition and integrity of the highly polar surface metal oxide layer has been considered critical for adequate bond strength. Adhesive primers have been shown to be capable of chemical bonding to base metal alloys.⁴

Surface treatments produce alterations in the surface texture of the alloy that may affect the contact surface area which is available for mechanical and chemical bonding. Although 2-D surface profilometry is readily available, the concept of 3-D surface profilometry to study the surface texture has been developed recently. The surface morphology of alloy can be altered depending on the surface treatment. However 3-D surface texture assessment after different surface treatments for RPD alloys is sparsely documented.⁷

Observing surface topography under higher magnifications using light microscopy and/or scanning electron microscopy has been included in previous studies.^{4,7,37} The treated alloy surfaces and/or the tested samples are visualized under magnification to qualitatively assess the surface topography and the modes of failure. Use of surface profilometry and scanning electron microscopy (SEM) can aid in interpretation of the test results.

With regard to the assessment of the fundamental behavioral properties of adhesive interfaces, there is general consensus that failure in shear occurs at lower stress than failure in tension. Hence a shear bond strength test that

genuinely assesses the resistance of the adhesive interface to shear stresses is considered as acceptable.¹²

In-vitro studies, at best can only be used as an indication of the clinical situation. Water storage and thermocycling are methods for evaluating bond durability of metal-resin bonded systems in in-vitro studies.⁵⁰ The thermocycling water bath subjects the samples to a combination of factors such as water moisture and temperature changes in an attempt to simulate conditions that are found intraorally and is an acceptable in-vitro method. Separate studies by Matsumara et al, Mudford et al and Smith et al, have considered the thermocycling procedure to be a satisfactory indicator to the effect of accelerated aging since, it causes fatigue at the alloy-acrylic resin joint interface and deterioration of the bond.^{18,32}

Studies evaluating the effects of various surface treatments on the bond strength of Co-Cr alloy to acrylic resin are well documented.^{4,6,29,57} Similar studies for titanium alloy, as applicable in removable partial dentures are relatively few.^{18,21,28} Studies comparing the shear bond strength of heat polymerized acrylic resin and Co-Cr and Ti-6Al-4V alloys incorporating a mesh design, subjected to different surface treatments and thermocycling along with a quantitative and qualitative surface analysis are lacking.

It is evident that the optimizing the shear bond strength between the alloy and acrylic resin interface is critical for the longevity of the prosthesis.⁶ Thus testing of shear bond strength of different partial denture alloys subjected

to various surface treatments prior to acrylisation holds clinical relevance and merits further research. Addition of aging and thermocycling parameters enhances the clinical reliability of the in-vitro results.

In light of the above considerations, the aim of the present in-vitro study was to comparatively evaluate the shear bond strength of heat polymerized acrylic resin to Co-Cr and Ti-6Al-4V alloys with two different surface treatments after being subjected to aging and thermocycling and correlated with quantitative 3-D surface texture analyses of treated alloy samples along with pre and post testing SEM analyses.

In this study, a custom-made mold was fabricated, to standardize the sample dimensions. Dunny, King et al¹³ tested nine acrylic retention designs for anterior edentulous spaces. They suggested that the strength of acrylic retention was directly proportional to the diameter of the metal spaces in the metal grid and recommended the large open-loop or bar network designs. Lee et al have shown that the open lattice design was prone for permanent deformation. They concluded that the surface treated mesh design was more retentive than surface treated lattice or bead design.²⁹ This was consistent with the results of Brown et al and Canay et al who demonstrated that retentive mesh was more effective in retaining acrylic resin than the lattice design.⁸ Hence in the present study, the mesh design was incorporated in the sample design.

A total of forty four samples were prepared of which 22 samples each were obtained from Co-Cr alloy and from Ti-6Al-4V alloy. Since cpTi is prone to deflection, Ti-6Al-4V alloy, ASTM Grade V was used in the present study as suggested in a previous study.^{21,37} The Co-Cr alloy samples were designated as Group I and the Ti-6Al-4V alloy samples were designated as Group II. The samples within the Groups I and II were further randomly divided into Groups Ia and Ib and Groups IIa and IIb. Groups Ia and IIa test samples were surface treated with air abrasion using 50µm alumina. Groups Ib and IIb test samples were surface treated with air abrasion using 50µm alumina followed by Alloy Primer application.

Ishii T, Koizumi H et al compared the influence of alumina abrasion pressures on bonding between an acrylic resin and two casting alloys. They recommended the application of alumina with a grit size between 50-70µm with 0.6 Mpa pressure for improved bonding of acrylic resin to the casting alloys. The SEM observation of this study showed that air abrasion created microroughening of the surface.¹⁵ Sharp B et al reported that air abrasion with 50µm grit size alumina particles cleans the alloy surface thereby improving the available surface area and wettability of the alloy surface, thus increasing the bond strength.⁴⁴ Hence air abrasion with 50µm was used as one of the test surface treatment procedures in this study.

Studies have shown that surface treatment with adhesive primer application improves the bond strength between alloys and acrylic

resin.^{4,16,36,58} Adhesive primers are capable of chemical bonding to base metal alloys due to the presence of functional monomers. Primers containing 10-methacryloxydecyl dihydrogen phosphate (MDP) and 4-methacryloxyethyl trimellitate anhydride (4-META) are considered effective for base metal alloys.⁶ Kim SS et al reported on the bonding of heat cure acrylic resin and Co-Cr and Ti alloy with two metal primers containing 4-META and MDP respectively and concluded that primer containing MDP is more effective at bonding than carboxylic primers such as 4-META.²¹ The 6-(4-vinylbenzyl-n-propyl)amino-1,3,5-triazine-2,4-dithione (VBATDT) molecule has been found to be an effective primer when used on noble metals.⁶ Kawaguchi et al, reported that the primer containing both MDP and VBATDT was effective to bond heat polymerized resin and cp titanium and Co-Cr alloy.¹⁸ Lim HP et al, reported that VBATDT had a significantly positive effect on the bond between the heat cured denture base resin and the base metal alloys.²⁸ Hence, Alloy Primer, a commercially available metal conditioning agent containing MDP and VBATDT was used in this study in conjunction with air abrasion as one of the surface treatment methods.

One randomly selected, representative surface treated alloy sample from each group was assessed quantitatively by surface texture analysis by 3-D non-contact surface profilometry and qualitatively for surface topography by SEM. Since all the samples in a particular test group were subjected to the same sample preparation procedures, it was considered justifiable to examine

only a single randomly selected sample from each group for surface roughness, in accordance with that followed in a previous study by Barclay et al.⁷ 3-D surface profilometry was chosen over a 2-D analysis, to obtain better 3-D visualization of the test surface as well as the average surface roughness value (Ra value). Further the non-contact 3-D surface profilometry procedure permitted the use of the same test sample for further investigations such as SEM, since the sample surface was not contacted by any probe or stylus. SEM of surface treated samples was done to assess the surface topography differences in line with previous studies.^{18,37,61}

After acrylisation, samples had a cylindrical acrylic extension to provide a means for holding the sample during shear bond strength testing as suggested in a previous study.⁶¹ The aging and thermocycling protocols followed in the present study were based on that suggested in the existing literature.^{42,51} Thermocycled samples were tested for shear bond strength testing using a universal testing machine. The mean shear bond strength values of each test group were statistically analyzed. Further, tested samples were subjected to qualitative analysis using SEM to assess the mode of failure is in line with previous studies.^{4,7}

In the present study, the mean shear bond strength value of Co-Cr alloy samples treated with air abrasion (Group Ia) was 2.5970 Mpa (Table 1) (Graph 1) and Co-Cr alloy samples treated with air abrasion followed by Alloy Primer application (Group Ib) was 6.7750 Mpa (Table 2) (Graph 2). The mean shear

bond strength value of Ti-6Al-4V alloy treated with air abrasion (Group IIa) was 1.6150 Mpa (Table 2) (Graph 3) and Ti-6Al-4V alloy treated with air abrasion followed by Alloy Primer application (Group IIb) was 5.3110 Mpa. (Table 4) (Graph 4)

On comparison between the mean shear bond strengths obtained for Co-Cr alloy samples, namely, Group Ia and Group Ib, the samples treated with air abrasion followed by Alloy Primer application showed a significantly higher bond strength than samples treated with air abrasion alone. (Group Ib > Group Ia) (Table 5) (Graph 7)

Similarly, on comparison between the mean shear bond strengths obtained for Ti-6Al-4V alloy samples, namely, Group IIa and Group IIb, the samples treated with air abrasion followed by Alloy Primer application showed significantly higher bond strength than samples treated with air abrasion alone. (Group IIb > Group IIa) (Table 6) (Graph 9)

Comparison of the mean shear bond strengths between the alloys showed the mean bond strength of Co-Cr alloy to be significantly higher as compared to Ti-6Al-4V alloy samples within each respective surface treatment. (Group Ia > Group IIa; Group Ib > Group IIb) (Tables 7 & 8) (Graphs 11 & 13)

Previous studies have used Alloy Primer application after air abrasion as one of the surface treatments either on Co-Cr alloy alone or in comparison

with noble or other base metal alloys. The primed surfaces were found to significantly increase the bond strength values for Co-Cr alloy.^{6,37,57} Kawaguchi et al concluded from a previous study that there was a significant improvement in the bond strength of acrylic resin to flat & non perforated samples of both Co-Cr alloy and cp titanium.¹⁸ The results of the present study are in line with those obtained from the previous studies. This can be attributed to the improved bonding between the acrylic resin due to the presence of functional monomers in the Alloy Primer metal conditioning agent.

The quantitative 3-D texture analysis shows that Co-Cr alloy samples surface treated with air abrasion (Group Ia) had an average surface roughness value of 0.514 μ m. Co-Cr alloy samples surface treated with air abrasion followed by Alloy Primer application (Group Ib) had an average surface roughness value of 0.672 μ m. Ti-6Al-4V alloy samples surface treated with air abrasion (Group IIa) had an average surface roughness value of 0.534 μ m. Ti-6Al-4V alloy samples surface treated with air abrasion followed by Alloy Primer application (Group IIb) had an average surface roughness value of 0.700 μ m. There was not much difference between the surface roughness value (Ra) between the alloys for any given surface treatment, although it is tempting to conclude that the softer the alloy, the rougher the grit blasted surface. Since only one representative test sample from each test group was

analyzed, statistical correlations between the surface roughness values could not be derived.

However 3-D and Advanced 3-D images of Groups Ib and IIb (surface treatment with air abrasion followed by Alloy Primer application) (Figs.66, 67, 70 & 71) showed a more evenly microroughened alloy surface with uniform distribution of peaks and valleys in contrast to Groups Ia and IIa (surface treatment with air abrasion alone) (Figs.64, 65, 68 & 69). This uniform surface texture could be attributed to adequate wetting of the air abraded surfaces by Alloy Primer, which in turn could have improved the bonding.

The qualitative analysis of surface topography of surface treated samples by SEM under 10x and 500x magnifications revealed a frosty & uniformly micro roughened surface with more number of well distributed peaks & valleys on the sample surfaces for Groups Ib and IIb (subjected to air abrasion followed by Alloy Primer application) (Figs.73, 75, 77 & 79) when compared to the surface topography of Groups Ia and IIa (subjected to air abrasion) (Figs. 72, 74, 76 & 78).

The qualitative evaluation of mode of failure of tested samples using SEM under 10x, 250x, 500x and 1000x magnifications, revealed a common picture for Groups Ia and IIa and Groups Ib and IIb respectively. For Groups Ia and IIa, the post testing alloy surface topography was similar to the initial pretest air abraded surface topography with few or no resin tags on the alloy

mesh surface and the post testing acrylic surface was comparatively smoother, these are suggestive of an adhesive failure between the alloy-acrylic resin interface. For Groups Ib and IIb, the post testing alloy surface topography revealed a heterogenous surface with distinct resin tags on the alloy surface and the post testing acrylic surface was roughened and fractured. These are suggestive of predominantly cohesive failure within the resin itself and some areas of mixed adhesive and cohesive failure.

The different failure pattern as observed by the SEM analysis of the fractured samples for the two different types of surface treatments can be linked to the significantly higher shear bond strength values obtained for samples treated with air abrasion followed by Alloy Primer application. These findings suggest that using chemical adhesives such as Alloy Primer in addition to air abrasion may be necessary for the long term success of the bond between the acrylic resin and alloy, irrespective of whether it were Co-Cr alloy or Ti-6Al-4V alloy. These findings are in consensus with those obtained from a recent study by Kawaguchi et al comparing surface treated and acrylicized Co-Cr alloy and cp titanium.¹⁸ However Ti-6Al-4V alloy was not included in that study. Other recent studies by Kim, Vang et al and Lim et al^{21,28} comparing the effect of adhesive primers on the shear bond strength of acrylic resin to Co-Cr alloy, cp Ti and Ti-6Al-4V alloy, have concluded that Alloy Primer significantly improved the bond strength. However, aging and thermocycling were not included in these study designs to draw more appropriate correlations with the results obtained from the present study.

Also in the above studies, Co-Cr samples showed superior bond strength as compared to both cp Ti and Ti-6Al-4V alloy for all the surface treatments tested. These findings are in line with those obtained from the present study. This can be attributed to the higher flexibility of Ti-6Al-4V alloy when compared to Co-Cr alloy which is inherently more rigid due to its composition.^{21,45} This is of particular clinical relevance since denture deflection during use can result in framework-resin debonding.³⁷ Thus special emphasis is needed in designing and fabricating stiff frameworks that can minimize denture deflection. In this regard, application of adhesive primers such as Alloy Primer can greatly enhance the bond strength and bond durability as is evident from the results obtained in the present study.

The present study was carried out as an in-vitro study. Though aging and thermocycling parameters were included in the study protocol, these were of shorter duration. Also not all in vivo conditions, such as the effect of cyclic loading were included in the study protocol. The effect of only one type of adhesive primer was tested. The results obtained in the present study must be interpreted with these limitations in mind. Future studies that include longer thermocycling duration, varied surface treatments and a detailed surface profilometric analysis are suggested to enhance the results obtained with the present study.

CONCLUSION

The following conclusions were drawn from the data obtained from the present in vitro study conducted to comparatively evaluate the shear bond strength of heat polymerized acrylic resin to Co-Cr and Ti-6Al-4V alloys with two different surface treatments after being subjected to aging and thermocycling and correlated with quantitative 3-D surface texture analyses of treated alloy samples along with pre and post testing SEM analyses.

1. The shear bond strength of heat polymerized acrylic resin to Co-Cr alloy samples treated with air abrasion after aging and thermocycling (Group Ia) showed a mean value of **2.5970Mpa**.
2. The shear bond strength of heat polymerized acrylic resin to Co-Cr alloy samples treated with air abrasion followed by Alloy Primer application after aging and thermocycling (Group Ib) showed a mean value of **6.7750Mpa**.
3. The shear bond strength of heat polymerized acrylic resin to Ti-6Al-4V alloy samples treated with air abrasion after aging and thermocycling (Group IIa) showed a mean value of **1.6150 Mpa**.
4. The shear bond strength of heat polymerized acrylic resin to Ti-6Al-4V alloy samples treated with air abrasion followed by Alloy Primer

application after aging and thermocycling (Group IIb) showed a mean value of **5.3110 Mpa**.

5. On comparison, the mean shear bond strength of the two Co-Cr alloy test groups treated with air abrasion (Group Ia, mean value- 2.5970 Mpa) and air abrasion followed by Alloy Primer application (Group Ib, mean value- 6.7750 Mpa) respectively, showed a statistically **significant difference (p-value<0.05)** with respect to each other.**(Group Ia<Group Ib)**
6. On comparison, the mean shear bond strength of the two Ti-6Al-4V alloy test groups treated with air abrasion (Group IIa, mean value-1.6150 Mpa) and air abrasion followed by Alloy Primer application (Group IIb, mean value-5.3110 Mpa) respectively, showed a statistically **significant difference (p-value<0.05)** with respect to each other. **(Group IIa<Group IIb)**.
7. On comparison, the mean shear bond strength of the two test groups, Group Ia (mean value-2.5970 Mpa) and Group IIa (mean value-1.6150 Mpa) treated with air abrasion, showed a statistically **significant difference (p-value<0.05)** with respect to each other. **(Group IIa < Group Ia)**.
8. On comparison, the mean shear bond strength of the two test groups Group Ib (mean value -6.7750 Mpa) and Group IIb (mean value- 5.3110 Mpa) treated with air abrasion followed by Alloy Primer application,

showed a statistically **significant difference (p-value<0.05)** with respect to each other. (**Group IIb<Group Ib**).

9. On overall comparison, the mean shear bond strengths of the four test groups, namely,

- ❖ Group Ib (air abrasion followed by Alloy Primer application- Co-Cr alloy): highest mean shear bond strength.
- ❖ Group IIb (air abrasion followed by Alloy Primer application- Ti-6Al-4V alloy): high mean shear bond strength.
- ❖ Group Ia (air abrasion- Co-Cr alloy): moderate mean shear bond strength.
- ❖ Group IIa (air abrasion - Ti-6Al-4V alloy): least mean shear bond strength.

GroupIb >Group IIb > GroupIa > Group IIa

10. Quantitative evaluation of the surface texture of the surface treated Co-Cr alloy test samples, namely, Groups Ia and Ib using 3-D non-contact surface profilometry revealed the following:

- ❖ The average surface roughness value (**Ra value**) for Group Ia representative test sample was **0.514µm**.
- ❖ 3-D and advanced 3-D images for Group Ia representative test sample showed irregular distribution of peaks and valleys on the alloy surface.

- ❖ The average surface roughness value (**Ra value**) for Group Ib representative test sample was **0.672 μm** .
- ❖ 3-D and advanced 3-D images for Group Ib representative test sample showed uniformly distributed and well defined peaks and valleys throughout the alloy surface.

11. Quantitative evaluation of the surface texture of the surface treated Ti-6Al-4V alloy test samples, namely, Groups IIa and IIb using 3-D non-contact surface profilometry revealed the following:

- ❖ The average surface roughness value (**Ra value**) for Group IIa representative test sample was **0.534 μm** .
- ❖ 3-D and advanced 3-D images for Group IIa representative test sample showed patchy distribution of peaks and valleys on the alloy surface.
- ❖ The average surface roughness value (**Ra value**) for Group IIb representative test sample was **0.700 μm** .
- ❖ 3-D and advanced 3-D images for Group IIb representative test sample showed even distribution of peaks and valleys on the alloy surface.

12. The qualitative evaluation of the surface topography of Co-Cr alloy samples (Group Ia and Group Ib) subjected to two different surface treatments by scanning electron microcopy under 10x and 500x magnifications, revealed a frosty and uniformly micro roughened surface

with more number of well distributed peaks and valleys on the sample surface of Group Ib as compared to that of Group Ia.

13. The qualitative evaluation of the surface topography of Ti-6Al-4V alloy samples (Group IIa and Group IIb) subjected to two different surface treatments by scanning electron microcopy under 10x and 500x magnifications, revealed a uniform frosty appearance, with micro abraded surface topography showing well defined peaks and valleys on the sample surface of Group IIb as compared to that of Group IIa.

14. The qualitative evaluation of the mode of failure of the tested samples (Group Ia, Group Ib, Group IIa and Group IIb) scanning electron microcopy under 10x, 250x, 500x and 1000x magnifications revealed the following:

- ❖ Group Ia – exhibited a predominantly adhesive failure pattern at the alloy-acrylic resin interface as observed on both the alloy and acrylic portions of the fractured test sample.
- ❖ Group Ib – exhibited a mixed adhesive and cohesive failure, with a predominantly cohesive failure pattern within acrylic resin, as observed on both the alloy and acrylic portions of the fractured test sample.

- ❖ Group IIa – revealed a predominantly adhesive failure pattern at the alloy-acrylic resin interface as observed on both the alloy and acrylic portions of the fractured test sample.
 - ❖ Group IIb – revealed a mixed cohesive and adhesive failure, with a predominantly cohesive failure pattern within acrylic resin, as observed on both the alloy and acrylic portions of the fractured test sample.
15. Among the two alloy samples tested, namely, Co-Cr alloy and Ti-6Al-4V alloy, samples subjected to surface treatment with air abrasion followed by Alloy Primer application showed significantly higher shear bond strength values than the samples subjected to surface treatment with air abrasion alone, as correlated with 3-D surface profilometric and scanning electron microscopic images.
 16. Co-Cr alloy test samples showed significantly higher shear bond strength values as compared to Ti-6Al-4V alloy test samples within each of the respective types of surface treatment methods tested in the study.
 17. Acrylised Co-Cr alloy test samples subjected to air abrasion followed by Alloy Primer application (Group Ib), showed the highest shear bond strength value. This is in correlation with the 3-D surface profilometric and scanning electron microscopic images.

SUMMARY

The present study was conducted in vitro, to comparatively evaluate the shear bond strength of heat polymerized acrylic resin to Co-Cr and Ti-6Al-4V alloys with two different surface treatments after being subjected to aging and thermocycling and correlated with quantitative 3-D surface texture analyses of treated alloy samples along with pre and post testing SEM analyses.

To comparatively evaluate the effect of two different surface treatments on the shear bond strength of Co-Cr and Ti-6Al-4V alloys, a total of 44 samples with dimensions of 1cm x 1cm x 1.6 mm were obtained, of which 22 samples were obtained with Co-Cr alloy and 22 samples with Ti-6Al-4V alloy. The samples were divided into four groups comprising of 11 samples each. The groups were designated as Group Ia, Ib, IIa and IIb. For Groups Ia and Ib, Co-Cr alloy samples were subjected to air abrasion alone and air abrasion followed by Alloy Primer application respectively, prior to acrylisation with heat cure denture base resin. For Groups IIa and IIb, Ti-6Al-4V alloy samples were subjected to air abrasion alone and air abrasion followed by Alloy Primer application respectively, prior to acrylisation with heat cure denture base resin.

One representative surface treated alloy sample from each group was subjected to quantitative surface texture analysis using 3-D non-contact

surface profilometry and qualitative surface topography analysis using scanning electron microscopy. The remaining 10 samples from each group were acrylised and subjected to aging and thermocycling before being subjected to shear bond strength testing. After shear bond strength testing, one randomly tested sample was selected, for each test group and qualitatively analyzed by scanning electron microscopy to assess the mode of failure. The results obtained from the study were statistically analyzed using one way analysis of variance (ANOVA) and 'T' test.

The shear bond strength values of the four test groups were compared and found to be statistically significant with respect to each other. The Co-Cr alloy samples subjected to air abrasion followed by Alloy Primer application (Group Ib) showed the highest mean shear bond strength followed by the Ti-6Al-4V alloy samples subjected to air abrasion followed by Alloy Primer application (Group IIb) followed by the Co-Cr alloy samples subjected to air abrasion (Group Ia) followed by the Ti-6Al-4V alloy samples subjected to air abrasion (Group IIa) (Group Ib > Group IIb > Group Ia > Group IIa).

Quantitative and Qualitative evaluation of surface treated test samples of all four test groups revealed a more uniform surface texture and topography for Groups Ib and IIb as compared as Groups Ia and IIa. Qualitative analyses of tested samples revealed a predominantly adhesive failure pattern at alloy-acrylic resin interface for Group Ia and IIa samples. Group Ib and IIb

exhibited a mixed adhesive and cohesive failure pattern, with a predominantly cohesive failure within the acrylic resin.

In the present study, among the two different surface treatments, surface treatment with air abrasion followed by Alloy Primer application showed higher and statistically significant shear bond strength values as compared to surface treatment with air abrasion alone for both types of alloy tested. Among the two different alloys, Co-Cr alloy showed statistically significant higher shear bond strength values as compared to Ti-6Al-4V alloy within each respective surface treatment. The results suggest that surface treatment with air abrasion followed by Alloy Primer application plays a key role in the improvement of shear bond strength of both Co-Cr and Ti- 6Al-4V alloys to heat cure denture base resin. This is in correlation with the 3-D surface profilometric and scanning electron microscopic images. Test samples of Co-Cr alloy subjected to air abrasion followed by Alloy Primer application showed the highest shear bond strength values in this study. Future research focusing on enhancing the bond strength between heat polymerized acrylic resin and titanium alloy are recommended.

BIBLIOGRAPHY

1. **Ahmed Ali.** The shear strength of acrylic base to minor connector. Dent J 2009; 10; 367-375.
2. **Anusavice KJ.** Philip's Science of Dental Materials; 11th edition; 238-250, 455-458.
3. **Baltag I, Watnabe K.** Internal porosity of cast titanium removable partial dentures: influence of sprue direction on porosity in circumferential clasps of a clinical framework design. J Prosthet Dent 2002; 88;151-8.
4. **Banerjee S, Engelmeier RL.** In vitro tensile bond strength of Denture Repair Acrylic resins to primed base metal alloys using two different processing techniques. J Prosthodont 2009; 18;676-683.
5. **Barclay CW, Williams R.** The tensile and shear bond strengths of conventional and 4-META self cure acrylic resin to different finishes of Co-Cr alloy. Eur.J Prosthodont Restor Dent 1994;3(1):5-9.
6. **Bulbul M, Kesim B.** The effect of primers on shear bond strength of acrylic resins to different types of metals. J Prothet Dent 2010; 103;303-308.
7. **Barclay WC, Spence D.** Micromechanical versus Chemical bonding between Co-Cr alloys and methacrylate resins. J Biomed Mater Res Part B: Appl Biomater 2007;81B; 351-357

8. **Brown DT, Desjardins RP.** Fatigue failure in acrylic resin retaining minor connectors. *J Prosthet Dent* 1987;58;329-335.
9. **Boucher LJ and Renner RP.** Removable Partial Dentures. Quintessence Publications, Chicago, Tokyo.76-77.
10. **Canay S, Hersek N.** Effect of 4-META adhesive on the bond strength of different metal framework designs and acrylic designs. *J Oral Rehabil* 1997;24:913-919.
11. **Crim GA, Swartz MS.** Comparison of four thermocycling techniques. *J Prosthet Dent* 1985;53;50-53.
12. **Curtis RV, Watson TF, Van Noort R.** Dental biomaterials Imaging, testing and modeling. Woodhead Publishing and Maney Publishing of The Institute of Materials, Minerals and Mining, CRC Press LLC, Florida, USA.309
13. **Dunny AJ, King GE.** Minor connector designs for anterior acrylic resin bases: A preliminary study. *J Prosthet Dent* 1975;34;496- 502.
14. **Eliopoulos D, Zinelis S.** Porosity of cpTi castings with four different casting machines. *J Prosthet Dent* 2004;92;377-381.
15. **Ishii T, Koizumi H.** Effect of alumina air abrasion on mechanical bonding between an acrylic resin and casting alloys. *Journal of oral science* 2009;51;161-166.

16. **Jacobson TE, Chang JC.** Bond strength of 4-META acrylic resin denture base to cobalt chromium alloy. *J Prosthet Dent* 1988; 60; 570-576.
17. **Kaiser DA.** Shear bond strengths and scanning electron microscope evaluation of three different retentive methods for resin- bonded retainers. *J Prosthet Dent* 1988;59:568-573.
18. **Kawamaguchi T, Shimzu H.** Effect of surface preparation on the bond strength of heat polymerized denture base resin to commercially pure titanium and cobalt chromium alloy. *Dental Materials Journal* 2011; 30(2);143-150.
19. **Kwon TY, Imai Y.** Influence of molecular weight of PMMA/MMA-TBB resin on durability of adhesion to titanium against thermal stress in water. *Dental materials Journal* 2006; 25(2); 291-296.
20. **Kim JY, Pfeiffer P.** Effect of laboratory procedures and thermocycling on the shear bond strength of resin-metal bonding systems. *J Prosthet Dent* 2003;90:184-189.
21. **Kim SS, Vang MS.** Effect of adhesive primers on bonding strength of heat cure denture base resin to cast titanium and cobalt-chromium alloy. *J Adv Prosthodont* 2009; 1:41-46.
22. **Kononen M, Rintanen J.** Titanium framework removable partial denture used for patient allergic to other metals: A clinical report and literature review. *J Prosthet Dent* 1995;1;1-4.

23. **Kourtis G.** Bond strengths of resin- to- metal bonding systems. *J Prosthet Dent* 1997;78:136-145.
24. **Kuphasuk C, Oshida Y.** Electrochemical corrosion of titanium and titanium based alloys. *J Prosthet Dent* 2001;85:195-202.
25. **Lamstein A, Blechman H.** Marginal seepage around acrylic resin veneers in gold crowns. *J Prosthet Dent* 1956;6:706-709.
26. **Livaditis GJ.** Etched castings: an improved retentive mechanism for resin-bonded retainers. *J Prosthet Dent* 1982;47:52-58.
27. **Livaditis GJ.** A chemical etching system for creating micromechanical retention in resin- bonded retainers. *J Prosthet Dent* 1986;56:181-188.
28. **Lim HP, Kim SS.** Shear bond strength and failure types of polymethylmethacrylate denture base resin and titanium treated with surface conditioner. *Int J Prosthodont* 2010; 23: 246-248.
29. **Lee G, Engelmeier RL.** Force needed to separate acrylic resin from primed and unprimed frameworks of different designs. *J Prosthodont* 2010;19:14-19.
30. **May KB, Russell MM.** The shear bond strength of polymethylmethacrylate bonded to titanium partial denture framework material. *J Prosthet Dent* 1993;70: 410-413.
31. **May KB, Razzoog ME.** Silane to enhance the bond between polymethylmethacrylate and titanium. *J Prosthet Dent* 1995; 73:428-431.

32. **Mudford L, Curtis RV.** An investigation of debonding between heat cured PMMA and titanium alloy. *J Dent* 1997;25:415-421.
33. **Mukai M, Fukui H.** Relationship between sandblasting and composite resin-alloy bond strength by a silica coating. *J Prosthet Dent* 1995;74:151-155.
34. **Nabdalung D, Powers JM.** Comparison of bond strengths of denture base resin to nickel-chromium beryllium partial denture alloy. *J Prosthet Dent* 1997;78:566-573.
35. **Nabdalung D, Powers JM.** Effectiveness of adhesive systems for a removable partial denture alloy. *J Prosthodont* 1998;7:17-25.
36. **Nabdalung D, Powers JM.** Comparison of bond strengths of three denture base resins to treated nickel-chromium-beryllium alloy. *J Prosthet Dent* 1998;80:354-361.
37. **Okhubo C, Watanabe I.** Shear bond strengths of polymethylmethacrylate to cast titanium and Cobalt-Chromium frameworks using five metal primers. *J Prosthet Dent* 2000;83:50-57.
38. **Okhubo C.** Present status of titanium removable partial dentures- a review of the literature. *J Oral Rehabil* 2008; 35:706-714.
39. **Rodrigues S, Shenoy V.** The dental applications of titanium and its alloys: A review. *J Nepal Dent Assoc.* 2009;10:151-157.

40. **Rodrigues RCS, Riberio RT.** Comparative study of circumferential clasp retention force for titanium and cobalt-chromium removable partial dentures. *J Prosthet Dent* 2002; 88: 290-296.
41. **Rodrigues RCS, Faria ACL.** Comparative study of two commercially pure titanium casting methods. *J Appl Oral Sci.* 2010; 18(5): 487-492.
42. **Rudd KD, Morrow RM.** Dental laboratory procedures for removable partial dentures; Second edition; Mosby publications; 374-389.
43. **Sedburry D , Burgess J.** Tensile strengths of three chemical and one electrolytic etching systems for a base metal alloy. *J Prosthet Dent* 1992; 68:606-610.
44. **Sharp B, Morton D.** Effectiveness of metal surface treatments in controlling microleakage of the acrylic resin-metal interface. *J Prosthet Dent* 2000;84:617-622.
45. **Shimpo H.** Effect of arm design and chemical polishing on retentive force of cast titanium alloy clasps. *J Prosthodont* 2008;17:300-307.
46. **Shimzu H, Kutz KS.** Use of metal conditioners to improve bond strengths of autopolymerising denture base resin to cast Ti-6Al-7Nb and Co-Cr alloy. *J Dent* 2006; 34:117-122.
47. **Suzuki T, Takahashi H.** Bonding properties of heat polymerized resin to Ti- 6Al-7Nb alloy. *Dental Materials Journal* 2005; 24:530-535.

48. **Stewart KL.** Clinical removable partial prosthodontics; Third edition; MDMI publications, USA; 43-48, 450-468.
49. **Taga Y, Kawai K.** New method for divesting cobalt-chromium alloy castings: sandblasting with a mixed abrasive powder. *J Prosthet Dent* 2001;85:357-362.
50. **Tanaka T, Kamada K.** A comparison of water temperatures for thermocycling of metal-bonded resin specimens. *J Prosthet Dent* 1995;74:345-349.
51. **Tanaka T, Atsuta M.** Pitting corrosion for retaining acrylic resin facings. *J Prosthet Dent* 1979;42:282-291.
52. **Tanaka T, Fujiyama E.** Surface treatment of nonprecious alloys for adhesion fixed partial dentures. *J Prosthet Dent* 1986;55:456-462.
53. **Van Meerbeek B, Peumans M.** Relationship between bond strength tests and clinical outcomes. *Dental Materials Journal* 2010;26:100-121.
54. **Watanabe I.** Effect of sandblasting and silicacoating on bond strength of polymer-glass composite to cast titanium. *J Prosthet Dent* 1999;82:462-467.
55. **Yanagida H, Taira Y.** Adhesive bonding of titanium-aluminium-vanadium alloy with nine surface preparations and three self curing resins. *Eur J Oral Sci* 2003;111:170-174.

56. **Yamauchi M, Sakai M.** Clinical application of pure titanium for cast plate dentures. *Dental Materials Journal* 1988;7(1): 39-47.
57. **Yilmaz A, Akyul MS.** The effect of metal primer application and Nd-Yag laser irradiation on the bond strength between polymethylmethacrylate and co-cr alloy. *Photomed Laser Surg.* 2011;29:39-45.
58. **Yoshida K, Taira Y.** Effects of adhesive primers on bond strength of self curing resin to cobalt-chromium alloy. *J Prosthet Dent* 1997;617-620.
59. **Yoshida K, Taira Y.** Effect of adhesive metal primers on bonding a prosthetic composite resin to metals. *J Prosthet Dent* 1993;69:357-362.
60. **Zinelis S.** Effect of pressure of helium, argon, krypton, and xenon on the porosity, microstructure, and mechanical properties of commercially pure titanium castings. *J Prosthet Dent* 2000;84: 575-582.
61. **Zurasky EL, Steven E.** Improved adhesion of denture acrylic resin to metal alloys. *J Prosthet Dent* 1987;57:520-524.